# Towards a Translational Pain Model - Techniques and developments

Etemadi, Leila

2017

*Document Version:*
Publisher's PDF, also known as Version of record

[Link to publication](#)

*Citation for published version (APA):*
Etemadi, L. (2017). *Towards a Translational Pain Model - Techniques and developments*. [Doctoral Thesis (compilation), Department of Experimental Medical Science]. Lund University, Faculty of Medicine.

*Total number of authors:*
1

*Creative Commons License:*
Unspecified

# Towards a translational pain model
## Techniques and Developments

LEILA ETEMADI | FACULTY OF MEDICINE | LUND UNIVERSITY 2017
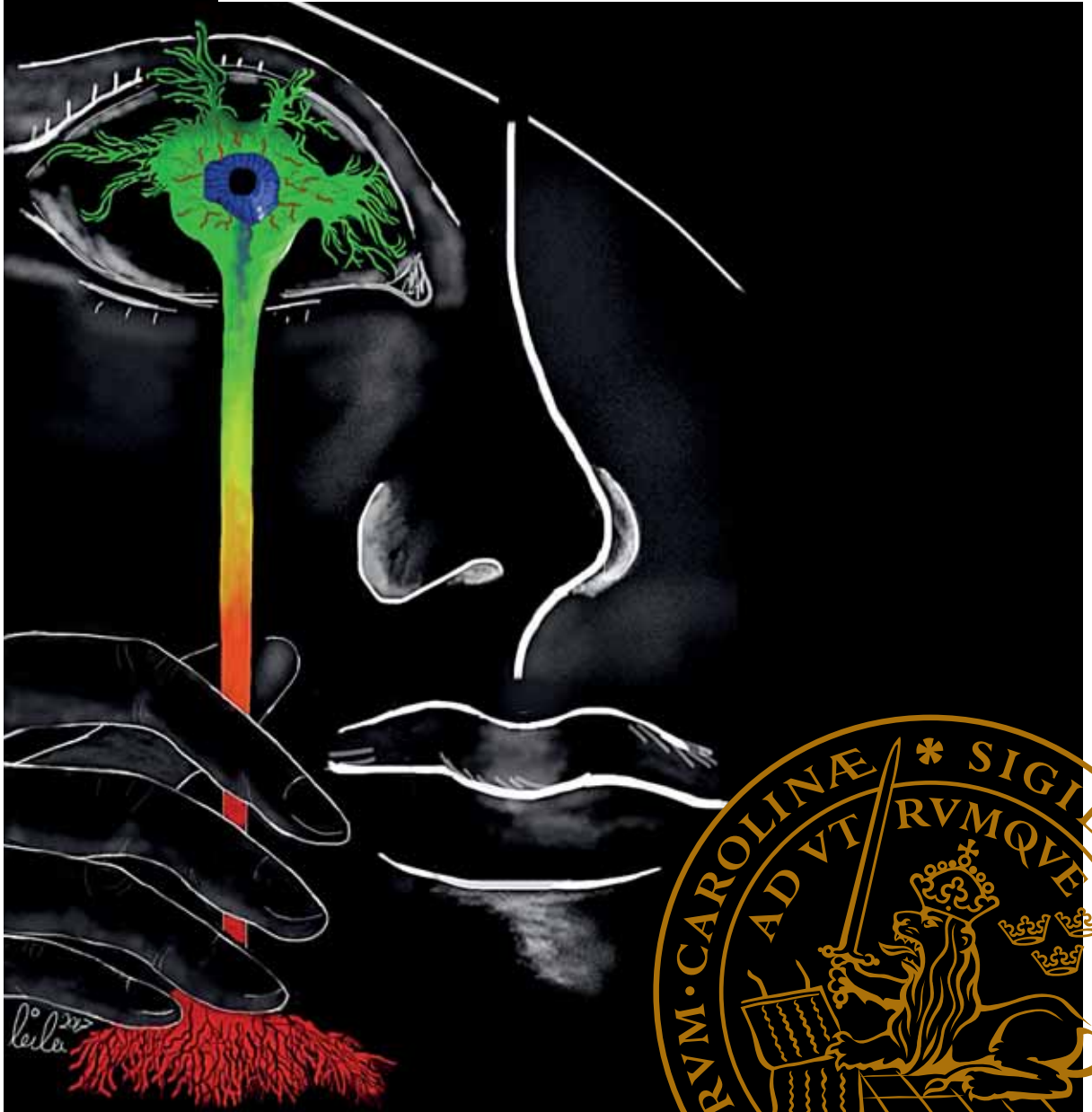
Towards a Translational Pain Model

# Towards a Translational Pain Model

## Techniques and developments

Leila Etemadi



LUND
UNIVERSITY

DOCTORAL DISSERTATION
by due permission of the Faculty of Medicine, Lund University, Sweden.
To be defended in Segerfalksalen, A-huset, BMC, April 27, 2017 at 13.15.

*Faculty opponent*
Professor Sven Tågerud

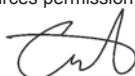| Organization | Document name |
|---|---|
| LUND UNIVERSITY<br>Faculty of Medicine<br>Department of Experimental Medical Science<br>Neuronano Research Center (NRC) | DOCTORAL DISSERTATION |
| | Date of issue<br>April 27, 2017 |
| Author Leila Etemadi | Sponsoring organization |

| Title and subtitle |
|---|
| Towards a Translational Pain Model - Techniques and developments |

**Abstract**

Pain is a major health issue for each affected individual and has a large impact on health costs. Most of our knowledge about this defensive system rely on data from different animal experiments. There is an obvious need for a translational pain model allowing comparisons between experimental animals and humans. UVB irradiation of skin has been introduced as a valid translational pain model and this model have resulted in comparable behavioral and electrophysiological data obtained from animals and humans. This thesis partly focus on detecting alterations for two neuropeptides (galanin and substance P), known to be involved in pain modulation, in the rat sensory nervous system after UVB irradiation of the rat hind paw on one side. UVB irradiation induced increased immunoreactivity for galanin in the lateral spinal nucleus (LSN) and in the dorsal horn of the rat spinal cord and also a reduction of the proportion of galanin positive neurons in corresponding DRGs. The changes observed for galanin in the LSN area have previously not been reported. The peak of the changes occurred 24 - 48 h after UVB irradiation which correlates with the time frame when primary and secondary hyperalgesia can be observed in rats and humans after UVB irradiation. UVB irradiation also induced increased c-fos activity in the dorsal part of the spinal cord and in the area around the central canal. For the other neuropeptide, substance P, an increase was observed 48 h in the LSN area. The changes observed on the ipsilateral side could also be observed on the contralateral side. This observation implies that the contralateral side should not be used as the control after induced inflammation on one side. Another goal of this thesis was to develop a mechanically flexible electrode system that precisely could target neurons deep in the brain. An electrode system containing 28 individual recording electrodes was constructed and it could be implanted into the brain after gelatine embedding. This electrode system made it possible to obtain stable neurophysiological recordings during eight weeks in awake, freely moving rats. Histological examination verified that the individual electrodes had reached their target, the subthalamic nucleus, and that they also spread out within the target. This electrode system can be used as a tool for further experimental pain studies. The fourth article focus on visualising neurons in histological sections from cortex, spinal cord and DRG using two pan-neuronal markers, HuC/HuD and NeuN. Different staining procedures were used, glass mounted sections or free floating ones with or without an antigen retrieval protocol. The anti-HuC/HuD antibody together with a standard immunohistochemical protocol worked well for cortical sections stained on glass or in a free floating mode. For the anti-NeuN antibody the best results were obtained after an antigen retrieval protocol. For spinal cord sections the use of the anti-HuC/HuD antibody gave the most favourable results. This antibody was used when the spinal cord sections were stained for evaluating the changes induced in the dorsal part of the spinal cord after UVB irradiation. Both antibodies worked well for DRG sections. In summary, this thesis demonstrates that UVB induced skin inflammation will cause rapid biochemical alterations in the parts of the nervous system related to pain signalling. A novel electrode system has been developed that can be used for further experimental pain studies. Furthermore, different pan-neuronal markers differ in their ability to stain neurons from different parts of the nervous system.

| Key words: UVB irradiation, pain, neuropeptides, inflammation, contralateral, lateral spinal nucleus, micro-array electrodes, pan-neuronal markers, immunohistochemistry |
|---|

| Classification system and/or index terms (if any) |
|---|

| Supplementary bibliographical information | Language: English |
|---|---|

| ISSN and key title: 1652-8220 | ISBN: 978-91-7619-436-2 |
|---|---|

| Recipient's notes | Number of pages 144 | Price |
|---|---|---|
| | Security classification | |

Signature                                  Date 2017-03-13

# Towards a Translational Pain Model

## Techniques and developments

Leila Etemadi

*Dedicated to*

*My Mom and My youngest brother*

کی رفته‌ای زدل که تمنا کنم تو را      کی بوده‌ای نهفته که پیدا کنم تو را

غیبت نکرده‌ای که شوم طالب حضور      پنهان نگشته‌ای که هویدا کنم تو را

*Poetry from*
**Foroughi Bastami**

# Content

# Abbreviations

| | |
|---|---|
| CGRP | Calcitonin gene-related peptide |
| DAPI | 4,6-diamidino-2-phenylindole |
| DRG | Dorsal root ganglion |
| i.p. | Intra-peritoneal |
| LCN | Lateral cervical nucleus |
| LSN | Lateral spinal nucleus |
| NKA | Neurokinin A |
| NK-1 | Neurokinin-1 |
| PBS | Phosphate buffered saline |
| PC | Parylene C |
| PCB | Plated circuit board |
| PAG | Periaqeuductal grey |
| PFA | Paraformaldehyde |
| Pt | Platinum |
| ROI | Region of interest |
| SC | Spinal cord |
| SNR | Signal to noise ratio |
| STN | Subthalamic nucleus |
| SP | Substance P |
| UVB | Ultraviolet B |

# Original papers included in this thesis

**Paper I:**

**Leila Etemadi**, Lina M.E. Pettersson, Nils Danielsen. UVB irradiation induces rapid changes in galanin, substance P and c-fos immunoreactivity in rat dorsal root ganglia and spinal cord. Peptides 87:71-83, 2017.

**Paper II:**

**Leila Etemadi**, Lina M.E. Pettersson, Nils Danielsen. UVB irradiation induces contralateral changes in galanin, substance P and c-fos immunoreactivity in rat DRG, dorsal horn and lateral spinal nucleus. Manuscript 2017.

**Paper III:**

**Leila Etemadi**\*, Mohsin Mohammed\*, Palmi Thor Thorbergsson, Joakim Ekstrand, Annika Friberg, Marcus Granmo, Lina M.E. Pettersson, Jens Schouenborg. Embedded ultrathin cluster electrodes for long-term recordings in deep brain centers. PLoS ONE 11(5):
e0155109, doi:10.1371/journal.pone.0155109, 2016. \*Shared first authorship

**Paper IV:**

**Leila Etemadi**, Lina M.E. Pettersson, Nils Danielsen, Cecilia Eriksson Linsmeier, Lina Gällentoft. Staining neurons in cortex, spinal cord and dorsal root ganglion using two different neuronal markers, HuC/HuD and NeuN. Manuscript 2017.

# Populärvetenskaplig sammanfattning

Smärta är ett allvarligt hälsoproblem som påverkar människors livskvalitet, men som också belastar hälso- och sjukvården. Studier har visat att ungefär 20% av befolkningen påverkas av smärta och att långvarig smärta kostar det svenska samhället 87,5 miljarder kronor per år (2006 års siffror).

Smärta kan uppstå efter olika typer av skador, t. ex efter skärskador, eller vid sjukdomar som reumatisk ledinflammation. Inflammation av olika slag är ofta förenat med smärta. De typiska tecknen på inflammation är just smärta, men också svullnad, rodnad, värmeökning och en försämrad funktion i det område som drabbats. Vid inflammation i t. ex. huden aktiveras särskilda nervtrådar som leder nervsignaler från det inflammerade området via ryggmärgen till ett särskilt område i hjärnbarken. Inflammation leder också till förändringar i själva nervsystemet, som förändringar i nervsystemets olika s.k. neuropeptider (små äggviteämnen) som anses vara inblandade i regleringen av smärtsvaret. I denna avhandling har två av dessa neuropeptider studerats, nämligen galanin och substans P, efter att huden på råttors ena baktass bestrålats med ultraviolett ljus, vilket åstadkommer en lätt "solbränna" och en inflammation i råtthuden. Galanin är en särskilt intressant neuropeptid då den anses både kunna fungera för att förstärka smärtsvaret för att senare motverka det. Denna djurmodell, bestrålning av hud med ultraviolett ljus, har visat sig särskilt användbar för att studera inflammatoriskt utlöst smärta då den ger jämförbara resultat mellan olika djur och människor. Den brukar räknas som en s.k. överförbar modell. Modellen har tidigare använts för att bevisa att smärta utlöst från ett inflammerat område ger en förstärkt smärtsignal, men förstärkning av smärtsignalerna kan även fås om hudområdet alldeles intill det inflammerade området smärtstimuleras.

I denna avhandling visas att bestrålning av hud ger inflammation genom att blodflödet i huden ökade till nästan det dubbla ett dygn efter bestrålningen. Denna hudinflammation ger mycket snabba förändringar (några timmar efter bestrålning) av neuropeptiden galanin i de områden av ryggmärgen och tillhörande nerver som anses vara inblandade i förmedling av smärtsignaler. Förändringar för galanin kunde även observeras i ett speciellt område av nervceller i ryggmärgen som normalt inte brukar studeras i liknande försök och som har en omtvistad roll i förmedlingen av smärtsignaler. Förändringarna för galanin inom detta omtvistade område i ryggmärgen har tidigare ej gjorts. För den andra neuropeptiden, substans P, var förändringarna mindre tydliga förutom i det speciella området av nervceller i ryggmärgen. Detta fynd styrker andra studier där förändringar av substans P studerats inom detta särskilda område.

Studierna visade också att förändringarna hos de båda neuropeptiderna uppstod i ryggmärgens båda sidor trots att bara den ena sidans tass bestrålats med ultraviolett ljus. Dessa fynd talar för att det finns kommunikation mellan de båda sidorna i nervsystemet på ryggmärgsnivå, vilket indikerar att inflammatoriskt utlöst smärta på den ena sidan leder till komplicerade reaktioner i nervsystemet. Sammanfattningsvis kan sägas, att de förändringar som observerades i denna avhandling korrelerar väl med andra studier på djur eller människa som använt samma inflammatoriska modell, bestrålning av hud med ultraviolett ljus.

I ett annat delarbete utvecklades ett flexibelt elektrodsystem innehållande 28 enskilda elektroder för att kunna registrera nervsignaler från djupt liggande strukturer i råttans hjärna. Genom en speciell teknik med inbäddning av alla elektroder i gelatin kunde detta flexibla elektrodsystem användas för att registrera nervsignaler från vakna, frigående råttor under åtta veckors tid. Gelatin tillför det flexibla elektrodsystemet stabilitet vilket möjliggör insättande av det i den relativt mjuka hjärnvävnaden och gelatinet kommer sedan att upplösas. Elektrodsystemet ger också möjlighet att sprida ut de olika enskilda elektroderna inom ett större område, vilket ger möjlighet att registrera signaler från fler enskilda nervceller. Systemet är så konstruerat att det kan anpassas för att registrera nervsignaler från olika hjärnstrukturer som anses vara inblandade i smärtsignalering. Det är ett nytt redskap som kan användas för att reda ut hur smärtsystemet fungerar.

I det sista arbetet märks nervceller med hjälp av olika antikroppar (äggviteämnen som mycket specifikt känner igen andra ämnen). De två använda antikropparna kan bara bindas in till nervceller och de markerade nervcellerna kan ses i vävnadssnitt genom att antikropparna har ämnen kopplade till sig som sänder ut ljus (fluorescerar) när vävnadssnittet belyses med ultraviolett ljus via mikroskopet. Syftet med detta delarbete var att reda ut vilken av antikropparna var mest lämplig för att markera nervceller i hjärnbarkssnitt (som innehåller många nervceller) eller i vävnadssnitt från ryggmärg eller från snitt från de anhopningar av nervceller som finns strax innan ryggmärgen. Olika typer av infärgningsrecept användes och infärgningen gjordes antingen på vävnadssnitt monterade på objektglas eller på vävnadssnitt som var friflytande och som senare monterades på objektglas. Resultaten visade att den ena antikroppen fungerade bättre för att detektera nervceller i vävnadssnitt från hjärnan och den andra antikroppen fungerade bättre för nervceller i vävnadssnitt från ryggmärgen. Det är viktigt att ha korrekta metoder för att markera nervceller i olika situationer, t. ex. vid studier där nervcellers närhet till olika elektroder är avgörande för att bestämma om en elektrod för registrering av nervsignaler fungerat eller ej.

# Abstract

Pain is a major health issue for each affected individual and has a large impact on health costs. Most of our knowledge about this defensive system rely on data from different animal experiments. There is an obvious need for a translational pain model allowing comparisons between experimental animals and humans. UVB irradiation of skin has been introduced as a valid translational pain model and this model have resulted in comparable behavioral and electrophysiological data obtained from animals and humans. This thesis partly focus on detecting alterations for two neuropeptides (galanin and substance P), known to be involved in pain modulation, in the rat sensory nervous system after UVB irradiation of the rat hind paw on one side. UVB irradiation induced increased immunoreactivity for galanin in the lateral spinal nucleus (LSN) and in the dorsal horn of the rat spinal cord and also a reduction of the proportion of galanin positive neurons in corresponding DRGs. The changes observed for galanin in the LSN area have previously not been reported. The peak of the changes occurred 24 - 48 h after UVB irradiation which correlates with the time frame when primary and secondary hyperalgesia can be observed in rats and humans after UVB irradiation. UVB irradiation also induced increased c-fos activity in the dorsal part of the spinal cord and in the area around the central canal. For the other neuropeptide, substance P, an increase was observed 48 h in the LSN area. The changes observed on the ipsilateral side could also be observed on the contralateral side. This observation implies that the contralateral side should not be used as the control after induced inflammation on one side. Another goal of this thesis was to develop a mechanically flexible electrode system that precisely could target neurons deep in the brain. An electrode system containing 28 individual recording electrodes was constructed and it could be implanted into the brain after gelatine embedding. This electrode system made it possible to obtain stable neurophysiological recordings during eight weeks in awake, freely moving rats. Histological examination verified that the individual electrodes had reached their target, the subthalamic nucleus, and that they also spread out within the target. This electrode system can be used as a tool for further experimental pain studies. The fourth article focus on visualising neurons in histological sections from cortex, spinal cord and DRG using two pan-neuronal markers, HuC/HuD and NeuN. Different staining procedures were used, glass mounted sections or free floating ones with or without an antigen retrieval protocol. The anti-HuC/HuD antibody together with a standard immunohistochemical protocol worked well for cortical sections stained on glass or in a free floating mode. For the anti-NeuN antibody the best results were obtained after an antigen retrieval protocol. For spinal cord sections the use of the anti-HuC/HuD antibody gave the most favourable results. This antibody was used when the spinal cord sections were

stained for evaluating the changes induced in the dorsal part of the spinal cord after UVB irradiation. Both antibodies worked well for DRG sections. In summary, this thesis demonstrates that UVB induced skin inflammation will cause rapid biochemical alterations in the parts of the nervous system related to pain signalling. A novel electrode system has been developed that can be used for further experimental pain studies. Furthermore, different pan-neuronal markers differ in their ability to stain neurons from different parts of the nervous system.

# Introduction

## Pain and inflammation

Pain is a major health issue which affects quality of life and also has a major impact on the health costs for a society. It has been estimated that the prevalence of pain is about 20% in the Swedish population and that the annual cost for long lasting pain is 87.5 billion SEK (Lundberg and Axelsson 2006). The International Association for the Study of Pain (IASP) has defined pain as 'an unpleasant sensory and emotional experience associated with an actual or potential tissue damage, or described in terms of such damage' (see web page for IASP Taxonomy).

Pain can be induced in different situations, one obvious situation is the direct tissue damage to the skin after a knife cut. Another cause is invading microorganisms which can induce inflammation that is followed by pain. Inflammatory pain can also be triggered by various autoimmune diseases such as rheumatoid arthritis and the induced inflammation will produce damage to the tissue and/or at the cellular level. The cardinal signs of inflammation are redness, heat, pain, swelling and impaired function. Furthermore, there will be alterations in local blood flow and vascular permeability, including release of trophic and growth factors from adjacent tissues, and an activation of the immune system. A consequence of inflammatory pain is that the perception of pain in response to non-noxious stimuli may be triggered (Das 2015, Dray 1995).

In brief, in response to peripheral tissue inflammation, two groups of nociceptor fibers, A∂-fibers and C-fibers, are transferring nociceptive signals from their free nerve endings through dorsal root ganglia (DRG) to the spinal cord. These free nerve endings are releasing various neuropeptides such as substance P (SP), calcitonin gene-related peptide (CGRP), neurokinin A (NKA) and galanin, locally. In the spinal cord, nociceptive information will be transmitted to the superficial layers of the dorsal horn, but also to lamina V (Craig 2003). In the spinal cord grey matter, the primary afferents connect either to interneurons or directly to the second order neurons in the spinal cord dorsal horn. The spinal cord dorsal horn lamina I contains neurons responding to noxious stimuli and the deeper layers contain neurons responding to both noxious and innoxious (harmless) stimuli

(Craig 2003, Craig and Dostrovsky 1991, Schnitzler and Ploner 2000). It is believed that these deeper located neurons have wide dynamic range properties. The axons from these two neuronal groups cross the spinal cord midline directly or after projecting one or two segments up or down and then continue cranially via the spinothalamic tract to the thalamus where they synapse. From the thalamus the third order neurons project to the pain perception areas in the cerebral cortex (Schnitzler and Ploner 2000). It is worth noticing, that some of dorsal horn neurons may expand their receptive fields, suggesting that they may develop a "wind up" effect producing cumulative or prolonged discharges (Das 2015, Herrero et al 2000).

# Lateral spinal nucleus

The current knowledge about the lateral spinal nucleus (LSN) is rather limited. However, there are reports suggesting its importance in pain modulation.

### Neuroanatomy and neurochemical profile

Rexed and Brodal (1951) were the first to describe a separate longitudinal cellular column in the cervical part of the cat spinal cord. This structure was named the lateral cervical nucleus (LCN). Further studies using rats showed a similar cellular structure extending throughout the entire spinal cord, and this was therefore called the lateral spinal nucleus (Gwyn and Waldron 1968). In rat, the LSN is localized in the white matter ventrolateral to the lateral part of the dorsal horn (Dagci et al 2008). This column of cells has also been identified in a number of species, in addition to the rat, e.g. in guinea pig, rabbit, ferret, and hedgehog (Willis and Coggeshall 1999).

Ultrastructural studies have shown that rat LSN neurons are of small multipolar, fusiform types ranging from 20 up to 35 μm. These neurons form an extended column underneath the pial surface of dorsolateral funiculus (Alvarez et al 2000, Giesler and Elde 1985, Gwyn and Waldron 1968, Rethelyi 2003) and for a simplified schematic drawing of the LSN connections see Fig. 1. The dendrites of these neurons have a different arborization pattern throughout the spinal cord. Some extend medially towards lamina I (Menétrey et al 1982), and others are reaching towards the pial surface (Brenshan et al 1984), and some even pass through the pia mater (Rethelyi 2003). This dendritic architecture supports the view that neurochemical alterations within the cerebrospinal fluid may influence the LSN neurons (Fig. 1). The presence of neuropeptides (vasoactive intestinal polypeptide, bombesin, dynorphin and SP) in some LSN neurons in the rat

lumbosacral segments was reported for the first time by Leah et al. (1988). These LSN neurons projected to the brain through different pathways including spinomesencephalic, spinoreticular and spinosolitary tracts.
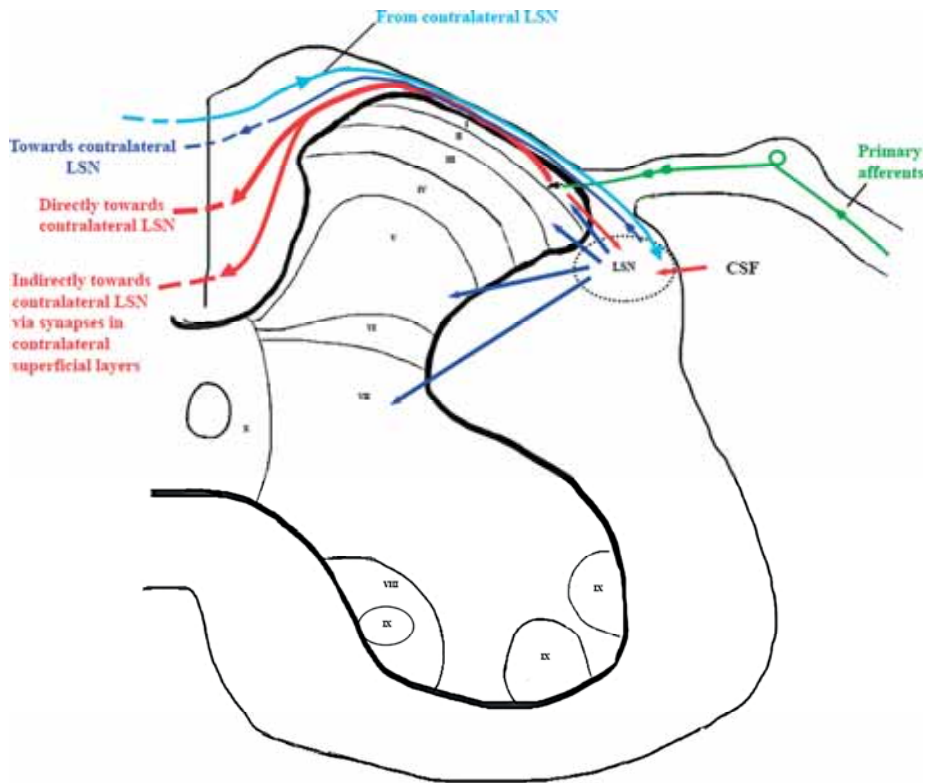


**Figure 1. Schematic drawing modified after Petkó and Antal (2000) and Rea (2009), summarizing the suggested projections to and from LSN in the lumbar part of the rat spinal cord.** Please note that the drawing does not reflect the exact anatomical configurations, it only points out the LSNs major efferent and afferent influences.

Primary sensory afferents (in green) are entering the spinal cord via the dorsal root and synapse with dorsal horn neurons in lamina I. The lamina I neurons (in red) project to both ipsi- and contralateral LSN. In addition, dendrites on LSN neurons arborize towards the pial surface and are suggested to register changes in the cerebrospinal fluid (in red). Furthermore, projections from LSN (in dark blue) are contacting neurons in lamina I, II, V and VII, as well as projecting to the contralateral LSN. The projections coming from the contralateral LSN are also indicated (in light blue).

## Role in nociception - brief overview

Rea (2009) reported that LSN receives nociceptive information in response to painful cutaneous thermal or chemical stimulations. Previous studies have reported that the LSN neurons project to brain structures involved in nociceptive processing, such as brain stem and different parts of the thalamus, hypothalamus and globus pallidus (Li et al 1997). Li et al (1997) pointed out that, since the limbic system is very important in pain and nociception, and projections from LSN and deeper dorsal horn laminae project to the limbic area these can be assumed to be involved in different pain features. At the spinal cord level, neurons from the LSN area project to the different laminae of the spinal cord including: laminae I, II, V and VII (Jansen and Loewy, 1997), Fig. 1. In 2009 a hypothesis was put forward that processing of peripheral noxious stimulation may start already at the spinal level, prior to processing at higher structures specialized on pain and nociception (Rea 2009).

After the discovery of certain neuropeptides within LSN neurons (Leah et al 1988), findings of nitric oxide (Nazli and Morris 2000, Valtchanoff et al 1992) and c-fos expression (Rea 2009) has been reported. Moreover, presence of the NK-1 receptor (Li et al 1998, Todd et al 2002), and glutamate vesicular transporter (Alvarez et al 2004) has also been detected in LSN area. The presence of SP is interesting since this neuropeptide is believed to be involved in pain and nociception. Several studies have demonstrated a high density of SP stained fibers in the rat LSN area (Gibson et al 1981, Ljungdahl et al 1978, Senba 1982). The SP found is considered to be produced in the adjacent dorsal horn (Bresnahan et al 1984, Ljungdahl et al 1978), or in the LSN itself (Chung et al. 1988), but is less likely to derive from the ipsilateral DRG (Bresnahan et al 1984).

Previous reports suggest that the LSN is involved in the pain pathway, but the present knowledge about the role of the different neuropeptides and receptors discovered in the LSN area is rather sparse (Mantyh et al 1995, Nazli and Morris 2000, Todd et al 2005, Valtchanoff et al 1992). Interestingly, significant changes in the contralateral LSN area has been reported in response to unilateral noxious stimulation (Rea 2009). It is assumed that this contralateral activation may be induced by two different pathways: i) axonal projections from lamina I neurons ipsilateral to the stimulated side, which are directly innervated by primary afferents from the periphery on the stimulated side (Grudt and Perl 2002, Olave and Maxwell 2004, Rea 2009, Todd et al 2002), or ii) indirectly by projections from the contralateral superficial layers of the spinal cord neurons, which in turn have been activated by commissural fibers from superficial dorsal horn neurons ipsilateral to the stimulated side (Petkó and Antal 2000), see Fig. 1.

# Inflammatory pain and neuropeptides

Neuropeptides are small peptides, which are produced mainly in the nervous system. These molecules are presumed to modulate the level of neuronal activity and they are involved in both peripheral and central processes, e.g. thermoregulation and inflammatory responses (for review see Carniglia et al 2017). The expression of neuropeptides is usually very plastic within the nervous system, and they respond to changes in the environment, such as nerve injury or inflammation. Neuropeptides coexist with classic neurotransmitters and have been described to have modulatory functions.

During inflammation, neurotrophins such as nerve growth factor increase the expression of some neuropeptides such as SP, NKA and CGRP within the sensory nerve endings. These neuropeptides will induce the release of other inflammatory mediators in the inflamed area by increasing the blood flow through vasodilation and plasma extravasation. Moreover, other neuropeptides such as galanin and somatostatin are thought to reduce afferent fiber excitability and consequently the neurogenically induced inflammatory response (Dray 1995).

The neuropeptide galanin is present in DRG neurons and in dorsal horn neurons and fibers (Liu and Hökfelt 2002). Galanin is described to be both a pro- and an antinociceptive agent in inflammatory pain. In fact, it is believed that the galanin family is involved in several physiological and pathophysiological conditions within the nervous system or other organs (Lang et al 2015). This neuropeptide has been described to have a role in metabolic and osmotic homeostasis, reproduction (Gundlach 2002), and also cognition (Kinney et al 2002). Galanin is also expressed in dopaminergic or GABAergic neurons in different parts of the nervous system (Lang et al 2015). Peripheral inflammation will induce opposite reactions for galanin in DRG neurons versus the ones observed in the spinal cord dorsal horn. Inflammation will induce a reduction of the proportion of galanin containing neurons in the DRG, but an increase in galanin content in the spinal cord dorsal horn, indicating a release/export from the galanin afferents (Ji et al 1995 and reviewed in Liu and Hökfelt 2002). Another neuropeptide SP, presumably also involved in nociception, is also affected by peripheral inflammation. Peripheral inflammation will induce an increase of SP immunoreactivity in fibers in the dorsal horn (Kar et al 1994) and an increase of SP synthesis in DRG neurons (Noguchi et al 1988).

Since Hunt et al (1987) described the expression of the immediate early gene, c-fos, in spinal cord neuronal structures in response to sensory stimulation there have been several reports demonstrating the induction of c-fos in various parts of the nervous system after noxious stimulations. However, it is important to be cautious about the relevance of induced c-fos expression after painful stimuli since

there are contradictory evidence pointing out that c-fos expression may occur also in response to other stimuli than nociceptive stimuli (Harris 1998).

# Contralateral controls, good or bad?

Anatomical studies using different species, including primates, have shown that spinal cord dorsal horn fibers cross and synapse with contralateral neurons located in different layers of the dorsal horn. In a study conducted by Szentágothai (1964), using histological techniques, it was reported that neurons located in the dorsal horn substantia gelatinosa projected to the contralateral substantia gelatinosa in cats and dogs. Several other studies have confirmed the presence of cross-communication between both sides of the spinal cord and that these projections can induce contralateral changes (Grubb et al 1993, Petkó and Antal 2000, Shenker e al 2003). However, it is not uncommon to use the contralateral side as the control in experiments where one side of the nervous system is damaged or only one side is subjected to induced inflammation (Koltzenburg et al 1999). The use of the contralateral side as the control can be questioned. For instance, in comparison with intact animals the number of neurons with bilateral receptive fields increases as a result of unilateral inflammation (Grubb et al 1993, Solodkin et al 1992). Moreover, evidence suggest that the LSN receive projections from both sides of the superficial layers of the spinal cord dorsal horn (Olave and Maxwell 2004, Petkó and Antal 2000, Rea 2009), potentially resulting in a contralateral effect there as well.

# Inflammatory pain models

At present, animal pain models are the major source for investigation about new forms of pain management (Woolf et al 2010). The problem is how different animal pain models can be translated to the human situation. Most of the animal models rely on different behavioral parameters. Furthermore, there are differences between laboratory animals and humans with regards to cortical development and different physical and behavioral signs and all animal pain models have ethical issues (Le Bars et al 2001). There are several established methods used to induce inflammatory pain, such as subcutaneous injections of formalin (Dubuisson and Dennis 1977), or injection of carrageenan or mustard oil. These are all invasive methods and produce complex behavioral patterns (Le Bars et al 2001). There is a need for a translational pain model that can be used in animals as well as in humans (O'Neill et al 2015), a method which will allow assessments in awake,

freely moving animals and that is not influenced by different motor responses (Ljungquist et al 2016).

During the last years, Ultraviolet B (UVB) irradiation has been introduced as a dose-related inflammatory pain model, in which the intensity may be adjusted. This model has provided comparable behavioral and electrophysiological results in both humans and animals (Bishop et al 2007, Bishop et al 2009, Di Giminiani et al 2014, Gustorff et al 2013, Ljungquist et al 2016, O'Neill et al 2015, Rukwied et al 2008). In fact, Ljungquist et al (2016) reported a significant increase of neuronal activity in the primary somatosensory cortex in freely moving rats after stimulating the UVB irradiated skin area using localized $CO_2$ laser stimulation, but also when the adjacent skin area was stimulated using the same type of stimulus. The findings in rats (Ljungquist et al 2016) occurred with a similar temporal pattern as those reported for humans after experimental UVB irradiation (Gustorff et al 2013). The previous concept has been that UVB irradiation only induce development of primary hyperalgesia. However, in the rat UVB model, the development of both primary and secondary hyperalgesia could be detected (Ljungquist et al 2016). The IASP definition of hyperalgesia is "increased pain from a stimulus that normally provokes pain" (see web page for IASP Taxonomy).

Furthermore, it has been reported that UVB irradiation destroys epidermal keratinocytes (Saade et al 2008), produces immunosuppression (Seiffert and Granstein 2002) and also creates a local and central inflammatory response, which is detectable in human (Bishop et al 2009, Gustorff et al 2013), rat (Bishop et al 2010, Eschenfelder et al 1995) and pig (Di Giminiani et al 2014, Rukwied et al 2008) skin. UVB irradiation of skin will also alter some of the pain related neurochemicals in the spinal cord (Bishop et al 2007, Polgar et al 1998). In summary, ultraviolet irradiation of skin can be considered a useful model for studying inflammatory pain in humans and laboratory animals (Lopes and McMahon 2016) and it is of interest to characterize this model in further detail.

# Electrodes

In order to understand the central nervous system during physiological and also during pathophysiological conditions it is necessary to be able to accurately record neurophysiological signals from neurons in the brain. Therefore, it is not surprising that the increasing development and construction of microelectrodes or even nano-sized electrodes (Suyatin et al 2013) for accurate electrophysiological recordings has been a quite intriguing subject for a variety of scientific fields, including medical science and microelectronic engineering (Liu et al 2012).

Various types of electrodes can also be used for stimulation of brain neurons in order to reduce symptoms of disease. So far, deep brain stimulation using electrodes has been employed as an effective method for symptomatic treatment of some neurodegenerative diseases in humans, such as essential tremor (Benabid et al 1996), and Parkinson´s disease (Obeso et al 2001), and it is also considered useful for treatment of epilepsy (Hodaie et al 2002) and obsessive-compulsive disorders (Gabriëls et al 2003). Based on some of the critical criteria for these probes, such as biocompatibility, insertion properties (stiffness, flexibility), corrosion and integrity of the array over the time, different types of wire and silicon probes have been developed (Liu et al 2012). Proper mechanical support for implantation of flexible micro-wire array electrodes into the cortex can be achieved by embedding the array in gelatine (Lind et al 2010). This technique made it possible to perform chronical recordings from the somatosensory cortex in freely moving animals after UVB irradiation of the rat hind paw (Ljungquist et al 2016). Even though our knowledge and technologies for manufacturing microprobes has improved substantially, there are still challenging issues to be explored; e.g. customising electrodes in order to reach to different anatomical areas of the brain (Buston and McIntyre 2006), how to get as close as possible to the target neuron(s), how to increase the probe length for targeting deeper areas without loosing target precision (Alivisatos et al 2012), and also to be able to reach the deeper areas of the brain with the possibility for 3D functionality recording of the electrode, and also to achieve high resolution recordings without increasing the size of the probe or inducing tissue damage (Du et al 2009).

# Staining neurons

Coons et al (1941) introduced immunofluorescence as a method for histological evaluation of sectioned tissue, a method that would be known as immunohistochemistry. In principal, this method is the meeting point for the following techniques: immunology, histology, and also chemistry. In brief, the method is visualizing an antigen – antibody complex by employing colour for light microscopy applications or using fluorochromes that will respond to ultraviolet lights. This method provides the possibility to label and study a variety of antigens and morphological structures in one section. Furthermore, in the 1990s antigen retrieval methods were introduced to increase the chances of detecting elusive antigens, where the fixation procedures had changed their tertiary protein structure (Ramos-Vara, 2005). When selecting markers (antibodies) for examination of different structures/cell types in the nervous system, e.g. neurons, one must consider if the selected marker is specific for staining of the selected cell type, i.e.

if it is capable of labelling all of the neurons without labelling other cells (Phillips et al 2004).

One of the pan-neuronal markers, which is commonly used to label myenteric neurons is the anti-HuC/HuD antibody. This neuronal marker was detected in human patients with a rare type of lung carcinoma, which was damaging their nervous system (Dalmau et al 1990, Denny-Brown 1948). Later a homologous family of Hu proteins (embryonic lethal abnormal visual or Elav) was discovered in Drosophila. This protein is involved in the development of the Drosophila nervous system and it has been suggested that any deficiency in the protein structure will cause death to the insect (Szabo et al 1991). The Hu-family contains at least three genes; HuC/ple21, HuD and Hel-N1, and the major differences are in the structure of their mRNA (Liu et al 1995).

Another commonly used neuronal marker is the anti-NeuN antibody. NeuN stands for Neuronal Nuclei, and this antibody has been considered a reliable neuronal marker over the years since introduced by Mullen et al (1992). In fact, Mullen et al (1992) named the protein detected by the monoclonal antibody mAb A60, NeuN. The function of the NeuN protein is still not fully understood. It has been reported that the NeuN marker is exclusively detecting neurons in all parts of the nervous system with some exceptions. Purkinje cells in the cerebellum, olfactory bulbar mitral cells, and photoreceptor cells were not detected (Mullen et al 1992). It is believed that the NeuN protein is produced in the early stages of embryogenesis within the post-mitotic neuroblasts (Gusel'nikova and Korzhevskiy 2015). However, there are also reports that NeuN antibodies might not be reliable markers for labeling spinal cord neurons in aging rats (Portiansky et al 2006).

A reliable neuronal marker is essential for the evaluation of neuronal density in a electrophysiologically relevant area, i.e. in the immediate area around an implanted electrode essential to achieve useful and reliable neurophysiological signals (Buzsáki 2004, Köhler at al 2015), but also for identification of neurons when studying the changes in various neurochemicals such as neuropeptides after inflammation or nerve injury.

# Aims

The overall aim of this thesis was to further characterise the translational pain model employing UVB irradiation of skin, but also to develop tools that can be used in experimental pain studies.

The specific goals were:

I.     To characterise biochemical changes in the sensory nervous system after UVB irradiation of rat skin using certain neuropeptides involved in inflammatory pain.

II.     To investigate if UVB irradiation of rat skin also induced changes on the contralateral side in the sensory nervous system.

III.     To develop and construct a mechanically flexible, multichannel electrode array, that could target deep brain structures and be used for further experimental pain studies.

IV.     To evaluate different staining protocols for visualising neurons in order to define which protocols/antibodies are best suited for staining neurons in different parts of the nervous system.

# General Methods and Protocols

In this section general methods used for the different studies in this thesis are described briefly, for details the reader is referred to the individual articles on which this thesis is based. In all different experiments, animals were kept under standard laboratory conditions, 12 h day/night, environmental 21°C temperature and they received food and water ad libitum. Experimental protocols were approved by the Lund/Malmö local ethical committee on animal experiments. The animals were weighed regularly for health condition evaluation. The Roman numbering refers to the different articles included in this thesis.

## Animals (I - IV)

In paper I - III female Sprague - Dawley rats, weighing 200 - 250 g (Taconic, Denmark) were used. In paper IV, rats weighing 350 - 450 g (Taconic, Denmark) were used. In paper I and II the animals were divided in 6 different groups; a control group (naïve animals, n = 4, in which both left and right side were evaluated), and five experimental groups (n = 8 per group). Five different times points after UVB irradiation (2, 12, 24, 48 and 96 h) was selected for perfusion and collecting spinal cord (SC):L5 and related dorsal root ganglia (DRG).

## UVB irradiation (I, II)

UVB irradiation were performed on anaesthetized animals, a mixture of fentanyl/midazolam (0.1 mg/kg, and 10 mg/kg respectively) was administered as a single intra-peritoneal (i.p.) injection. The specific choice of anaesthesia was based on its reported neutral influence on the expression of the selected markers, especially c-fos (Takayama et al 1994). The heel area of the right hind paw (Fig. 2) was exposed to UVB irradiation, 1.3 J/cm$^2$, from a narrow band PL-L/PL-S lamp (Phillips, UK, between $\lambda$ = 305–315 nm, kmax = 311 nm, double pins spaced 2.8 cm) producing an even field of irradiation. This level of UVB irradiation is under the blistering threshold (Ljungquist et al 2016).
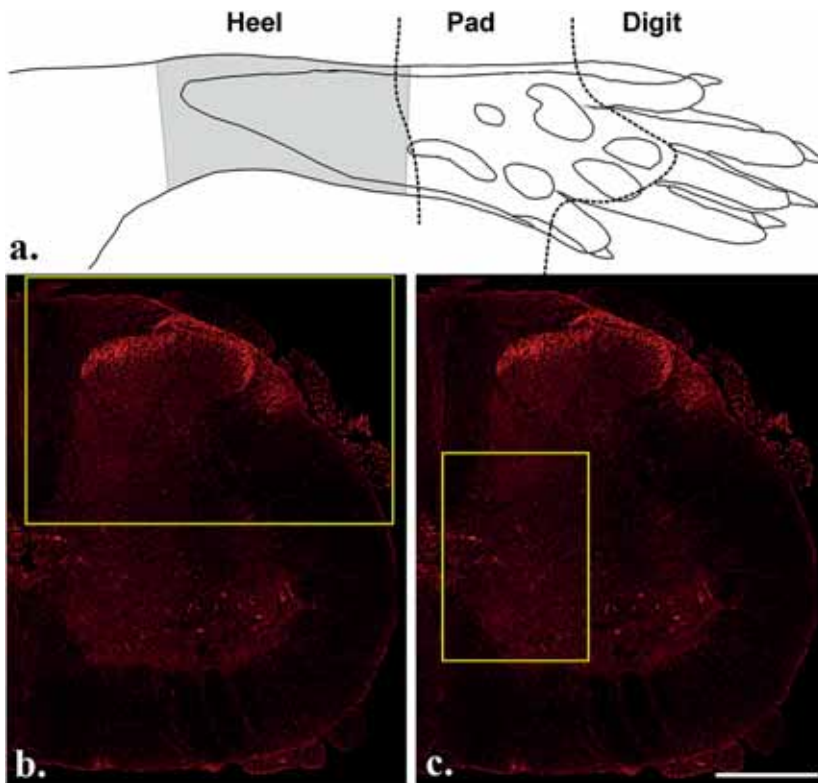
**Figure 2 Schematic picture of the rat hind paw indicating the UVB irradiated area and region of interests (ROIs).** Laser Doppler values are obtained from this area. Dotted lines are dividing the paw in three different areas: heel, pad and digit (a). In the spinal cord, the ROI:s used for quantification of immunoreactivity in the dorsal spinal cord area and area around the central canal are shown in (b) and (c) respectively. The large ROI (b) includes the dorsal horn and the LSN. Scale bar b and c = 500µm. Picture reproduced from Etemadi L., Pettersson L.M., Danielsen N. UVB irradiation induces rapid changes in galanin, substance P and c-fos immunoreactivity in rat dorsal root ganglia and spinal cord. Peptides, 2017. 87: 71-83; open access publication.

# Blood flow (I, II)

The intensity of UVB induced inflammation was determined by measuring cutaneous blood flow using laser Doppler flow meter (Moor-LAB, Moor Instruments, UK) technique in awake animals. The laser Doppler probe was attached to the irradiated area, which is a hairless area and will allow for proper attachment of the probe. Blood flow data were obtained from irradiated paws just before and 24 h after UVB irradiation. These readings were then compared to data collected from contralateral paws as well as with data from a control group (naïve intact animals).

# Histology (I – IV)

## Tissue preparation, staining and immunohistochemistry

In paper I and II, animals were perfused 2, 12, 24, 48, or 96 h after UVB irradiation of the right hind paw. Animals received an i.p. overdose of fentanyl/midazolam injected as a single injection. In paper III and IV, animals were perfused after an overdose of pentobarbital (i.p., 200 mg/kg; Apoteket Product and Laboratories Incoch Laboratorier AB, Stockholm Sweden). All animals were subsequently transcardially perfused with ~150 ml of room tempered saline (0.9% NaCl in distilled water), followed by 300 ml of ice-cold 4% paraformaldehyde (PFA) in 0.1 M phosphate buffer (pH 7.4).

The brain (papers III and IV), spinal cord lumbar enlargement (SC: L5), and corresponding dorsal root ganglia (DRG:L5) (papers I, II and IV) were harvested, and post-fixed in 4% PFA over night (brain: papers III and IV), or for 1–2 h (DRGs and SC: papers I, II and IV). After this, tissues were cryoprotected in 25% sucrose solution until equilibrated, and sectioned onto SuperFrost® plus slides (Menzel-Gläser, Germany) at 16 μm (papers I and II), 20 μm (paper IV), and 30 μm (paper III) thickness using a cryostat (MicromGmbH, HM 560,Germany). During sectioning procedures, careful attention to the orientation of the tissues was taken. Slides were stored at −25°C prior to staining procedures which was performed at room temperature. In the final step, slides were cover slipped using polyvinyl alcohol with DABCO® (Fluka/Sigma-Aldrich, Switzerland) for Cresyl violet staining (paper III), and DPX mounting media (Fluka, Germany) for immunostained slides (papers I, II, and IV).

In paper III, brain sections were stained with Cresyl violet. In brief, frozen sections were rinsed in ethanol/chloroform (1:1) overnight at room temperature. The next day slides were rehydrated using ethanol (100%, 95%), rinsed in distilled water (2 minutes/step), stained with Cresyl violet (Life Science products & services company; 0.1% in 0.3% acetic acid in $dH_2O$; 5 minutes), rinsed in distilled water (1 minute), dehydration in ethanol (95%, and 2 x 100%), and xylene (2 x 100%, 5 minutes).

## Immunohistochemical staining of brain, spinal cord and DRG

For papers I-II standard immunohistochemical staining of glass mounted sections was performed. The sections were rinsed in phosphate buffered saline (PBS) (0.01 M, pH = 7.4), and incubated in a blocking solution (5% normal goat serum in 0.25% Triton X-100 in PBS), for 1 h at room temperature. The procedure was

followed by primary antibody incubation over night at room temperature. The following primary antibodies were used for staining in papers I and II: i) galanin, ii) substance P, iii) c-fos, and iv) HuC/HuD. The following day, slides were rinsed in PBS, and incubated with 4',6-diamidino-2-phenylindole (DAPI, a cell nuclear marker), goat anti-rabbit IgG Alexa 594, and goat anti-mouse IgG Alexa 488 (diluted in blocking solution) in light sealed incubation chambers for 2 h. At the end of the procedure, slides were rinsed in PBS and cover slipped using polyvinyl alcohol with DABCO® (Fluka/Sigma-Aldrich, Switzerland). For detailed information about the antibodies used, see Table I.

**Table I. Summary of primary and secondary antibodies and nucleic acid stain.**
These primary and secondary antibodies and nucleic acid are used for immunohistochemical staining of spinal cord and DRGs.

| Name | Host | Characteristics | Working dilution | Source |
|------|------|------|------|------|
| Galanin | Rabbit | Neuropeptide | 1:1000 | Cat. Nr. 7100(T-4326), Peninsula |
| Substance P | Rabbit | Neuropeptide | 1:1000 | Cat. Nr. 20064, Immunostar |
| c-fos | Rabbit | Protein: transcription factor | 1:10 000 | Cat. Nr. PC38, Calbiochem |
| HuC/HuD | Mouse | Neuronal marker | 1:600 | Cat. Nr. A-21271, Life technology |
| NeuN | Mouse | Neuronal marker | 1:100 | Cat. Nr. MAB377, Millipore |
| Alexa flour 594 | Goat | Goat anti-rabbit IgG (H+L) | 1:500 | Cat. Nr. A11005, Invitrogen |
| Alexa flour 488 | Goat | Goat anti-mouse IgG (H+L) | 1:500 | Cat. Nr. A11001, Invitrogen |
| DAPI | | Nucleic acid stain (4',6-diamidino-2-phenylindole) | 1:1000 | Cat. Nr. D3571, Invitrogen |

In paper IV sections were stained using one of two separate staining procedures; i) staining of free-floating sections, or ii) staining of glass mounted sections. Furthermore, in paper IV, two different staining protocols were used, a standard protocol (described above) or an antigen retrieval protocol. The antigen retrieval protocol for glass mounted section started with a hydration step in Tris-buffert (Sigma-Aldrich, Germany), then the sections were immersed in a 10 mM sodium citrate buffer (0.05% Tween 20, pH 6) and microwaved for 3 x 5 min at 500 Watt, rinsed in Tris-buffert and blocked with 5% normal goat serum in Tris-buffert. The slides were incubated overnight (room temperature) with mouse anti-NeuN (1:100) or mouse anti-HuC/HuD (1:600) diluted in Tris-buffert blocking solution. For secondary antibody staining, the standard protocol was followed but with some minor alterations, Tris-buffert was used instead of PBS and Triton-X100 was omitted from the blocking solution. For free-floating sections, antigen retrieval protocol was performed as described glass mounted sections and the sections were

mounted on glass slides after the final rinsing step. Thus for paper IV, eight separate groups were evaluated, four for the HuC/HuD antibody: 1) free-floating sections: standard staining protocol (FHS), 2) free-floating sections: antigen retrieval protocol (FHA), and 3) glass mounted sections: standard staining protocol (GHS) and 4) glass mounted sections: antigen retrieval protocol (GHA). The next four groups were for the NeuN antibody: 5) free-floating sections: standard staining protocol (FNS), 6) free-floating sections: antigen retrieval protocol (FNA), 7) glass mounted sections: standard staining protocol (GNS), and 8) glass mounted sections: antigen retrieval protocol (GNA). For DRG, only glass mounted sections were studied. For more details see Table II.

**Table II. Table outlining the different protocols used in paper IV and the number of images analysed for each part of the nervous system.** The abbreviations are used to identify the different protocols (see above). Six histological images were analysed for cortex (one image for each protocol; for the spinal cord 12 images were analysed per protocol (one image from the dorsal and one from the ventral horn); and for the DRG six images were analysed per protocol.

| Markers | HuC/HuD | | | | NeuN | | | |
|---|---|---|---|---|---|---|---|---|
| Abbreviation | FHA | FHS | GHA | GHS | FNA | FNS | GNA | GNS |
| Tissue handling | Free-floating | Free-floating | Glass mounted | Glass mounted | Free-floating | Free-floating | Glass mounted | Glass mounted |
| Protocol | Antigen retrieval | Standard | Antigen retrieval | Standard | Antigen retrieval | Standard | Antigen retrieval | Standard |
| Number of images analysed (cortex) | 6 | 6 | 6 | 6 | 6 | 6 | 6 | 6 |
| Number of images analysed (spinal cord) | 12 | 12 | 12 | 12 | 12 | 12 | 12 | 12 |
| Number of images analysed (DRG) | - | - | 6 | 6 | - | - | 6 | 6 |

## Image acquisition

Slides were examined and imaged under a microscope (Nikon Eclipse 80i, Japan), using light microscopy (paper III) or fluorescence microscopy (papers I, II, and IV). A 10X objective was used to construct photomicrograph montages of DRG:L5 and SC:L5 (papers I and II), and a 20X objective for all other documentation and analysis (papers I and IV and the c-fos data in paper II). The microscope was connected to a DS-Ri1 digital camera (Nikon Instruments, Japan). Image capture and analysis were performed using the NIS-Elements 3.1 software (papers I and II), and 3.2 software (papers III and IV) (Nikon Instruments, Japan).

## Quantitative and qualitative analysis

In papers I and II, at least 6 DRG sections from each animal/experimental group was screened qualitatively, and then one representative section from each of the animals (i.e. 8 animals per experimental group) was evaluated quantitatively. In each representative section, at least 250 positive neuronal profiles positive for the neuronal marker HuC/HuD was counted. In the next step, the influence of UVB irradiation on the proportion of galanin, SP and c-fos immunopositive neurons in DRG was analysed and compared with the control group data. It was noted that changes in the proportion of galanin and SP immunoreactive neurons occurred, which triggered a further analysis with respect to eventual changes in neuronal size, i.e. whether the proportion changes induced were size dependent or not. The cell diameter for all of the counted cells in each DRGs were calculated from the neuronal profile cross-sectional areas, where only individual profiles containing a visible nucleus were selected for analysis. This procedure was only done in paper I. Neuronal profiles with diameters of <35 µm were defined as small-sized, and neurons with a diameter of ≥35 µm were considered as medium- to large-sized (Giuffrida and Rustioni 1992).

To quantify the density of galanin and SP expression in the dorsal part of the spinal cord lumbar enlargement at the L5 level six spinal cord-sections/animal and experimental groups (n = 4 for the control animals where both left and right sides were examined and n = 8 animals for each experimental condition) were quantified (papers I and II). The density of labelling was measured in specific regions of interest (ROI) in the photomicrographs and presented as a proportion of the total analysed area in the respective ROI. In papers I and II a larger ROI was used for the dorsal spinal cord area (ROI: 1200 × 1800 µm; which included the dorsal horn area and the LSN area), and a smaller ROI (ROI: 1000 × 700 µm) for the area around the central canal. For papers I and II the quantifications were performed by measuring the immunoreactive area (for galanin or SP) in relation to the entire ROI area. For paper IV a ROI with the dimension 250 × 250 µm was used for brain and spinal cord sections and the mean intensity or the signal/background ratio of the immunohistochemical staining within this ROI was determined for all different groups.

In paper I and II, the threshold for signal to background ratio for galanin immunofluorescence was set at 4.5 times above background and for SP immunofluorescence at 9 times above background intensity. The fraction of galanin or SP immunofluorescent area was subsequently determined above threshold. For paper IV, as the exposure time during image capturing differed between the two antibodies (NeuN = 33 ms and HuC/HuD = 67 ms), statistical comparisons were performed between the following groups: i) FHA, FHS, GHA, and GHS (HuC/HuD stained spinal cord or cortex, respectively), and between ii)

FNA, FNS, GNA, and GNS (NeuN-stained spinal cord or cortex, respectively), and between iii) GHA and GHS (HuC/HuD stained DRG), or between iv) GNA and GNS (NeuN-stained DRG).

For qualitative analysis of c-fos in papers I and II, one representative SC section from each animal per experimental group (n = 4 for the control group in which both left and right sides were examined and n = 8 for each experimental condition) was selected, and the distribution of c-fos immunoreactivity in two regions was evaluated: i) the dorsal part of the spinal cord and ii) the area around the central canal. The photomicrographs of the spinal cord sections stained for c-fos, captured under a 20X objective, were scored with regards to the presence of c-fos labelled neurons using a method for qualitative analysis modified from Olson et al (1993) where i) + (none or very few neurons immunoreactive for c-fos); ii) ++ (moderate number of c-fos positive neurons), and iii) +++ (more frequent neuronal staining of c-fos).

In paper IV, the qualitative scoring (the intensity of neuronal staining, detectability of the neurons, the level of background) was performed by scoring the histological images from 1 – 4 as follows: score 1 (signifying an histological stained section with almost none immunohistochemical staining signal), 2 (when the immunohistochemical staining signal was poor, the cells were well not defined, or the image quality did not allow for counting cells manually), 3 (immunohistochemical staining signal allowing for counting cells manually), and 4 (strong and well defined immunohistochemical staining signal).

# Fabrication and characterization of deep brain recording electrode (III)

## Probe fabrication

For probe manufacturing, pure platinum (Pt) temper annealed 12.5 μm micro-wires (Advent Research Material; England) was used as electrodes and they were insulated with Parylene C (PC) (dichloro dipara xylylene). The chosen insulation material is practically impermeable to moisture when an intact and pore free surface is achieved. It is frequently used for coating industrial medical devices were it has been shown to have a remarkable stability. It is anti-corrosive, tolerant to moist and ion-rich environments such as the human body and highly biocompatible (Schmidt et al., 1988). After coating the Pt wires with PC (for detailed information about the parylenisation process, see paper III), the quality of the PC surface (smoothness, cracks or holes) and homogenous thickness (4 ±

1μm), as well as the impedance, was evaluated using a scanning electron microscope (SEM) (SU1510-ver1.0 model, Hitachi High-technology corporation, Japan) for imaging and a Gamry Potentiostat (Series G300, Warminster, USA) for impedance measurements (for further details see Fig. 1 paper III). In the next step, twenty-nine PC coated, Pt-wires were soldered to a printed circuit board (PCB) with 30 gold-plated pads, one considered to be a local reference, and the 28 remaining Pt-wires as recording electrodes during the data acquisition procedure. For animal ground, a non-insulated silver wire (diameter: 150 μm, Advent research materials Ltd, England) soldered to the PCB board was used. The tip of each individual PC coated electrode was de-insulated 25 μm up from the tip, and then the distal end was cut, using a high-precision laser (Standard micro-milling system, New Wave Research Class 1, USA) (for further details see paper III). The in vitro impedance was measured, at a frequency of 1kHz, for the electrode leads in the final probe using a Gamry potentiostat.

## Moulding of the probe

To be able to implant the thin and flexible probes in deep brain structures in a controlled manner, a Plexiglas mould was constructed in which it was intend to gather and embed all the ultrathin Pt-wires into a straight and stiff probe with a sharp tip. First, the electrode bundle was slowly dipped into a warm gelatine matrix (50°C) with a controlled speed of 1.2 cm/min, and after a drying pause for 1– 2 min, it was centred in the mould. For further embedding of the probe, a heated gelatine matrix solution was injected into the mould through a side channel. To optimize drying of the gelatine matrix, the mould containing the probe was stored in a humidor chamber with the relative humidity of 21% for 48 h. To increase the dissolution time of the gelatine matrix, the moulded probe was dip coated (dip speed 6 cm/min) two times in Kollicoat™ MAE 100P (Supplier: Sigma Aldrich Sweden AB (5% in absolute ethanol). Kollicoat™ is a dispersible polymer, often used as a film-forming agent in pharmaceutical products.

## In vitro dissolution test and evaluation of electrode spread

To examine the influence of the Kollicoat™ on gelatine dissolution and electrode spread, a series of in-vitro experiments were conducted. In short, dummy gelatine probes, i.e. gelatine needles moulded into the mould used for probe-fabrication without any internal electrodes, were produced as described above. In addition, Cresyl violet was added to the gelatine mixture to increase visualization of the probes.

For evaluation of dissolution insertion of two groups of gelatine embedded probes were examined; i) kollicoated (5%, 2 layers, n = 8), and ii) non-kollicoated controls (n = 7). The probes were inserted 7 mm into a tempered block of agarose (37°C, 0.5%, commonly used as an in vitro model for mimicking mechanical properties of the rat brain) with controlled speed (100 µm/sec; using a micromanipulator), and documented for 10 min.

The evaluation of spread was performed on kollicoated (2 layers, 5%) gelatine embedded probes. The final spread of the distal tips of the wires after insertion 8 mm into the agarose block (speed 100 µm/sec, insertion to 7 mm, wait 10 min, further insertion 1mm to final depth) was documented. The depth was chosen with consideration to the approximate target depth of the rat brain subthalamic nucleus (STN). The wires spread and formed a cluster of recording-sites at the target-depth, which was assessed from the documented images. Final spread was defined as the distance between the wire tips furthest apart.

*Mechanical testing of electrode wires*

Buckling testing of 10 mm long microwires was performed using materials testing machine (Zwick GmbH & Co. KG; Zwick/ Roell BDO- FBO. 5TH) with a load cell (Zwick/ Roell KAP-Z 5N), and acquisition system (Zwick/Roell testXpert II). For further details, see paper III.


# Probe implantation

Implantations were targeting the STN, a nucleus located ~8 mm deep into the rat brain. After stabilizing the head of the anesthetized animal in the stereotaxic frame, implantation was performed at the following co-ordinates in relation to bregma; AP: -3.6 mm, L = ± 2.4 mm, depth 7.8 mm. After removing the dura the electrode bundle was implanted into the brain using the same three-step procedure as describe above, i,e, i) insertion to 1 mm pre-target, speed 100 µm/sec, ii) wait 10 min, iii) further insertion to final target, speed 10 um/sec; for further details see paper III, Section 2.2). The ground wire was the wound around the stainless steel skull screws. The electrode/contact was anchored to the skull, using dental cement (GC FujiCEM2, GC Belgium, Europe). Rats received injections of Temgesic® to reduce postoperative pain as well as antidote to the anaesthesia, and were observed during the awakening phase.


# Neural recordings and data analysis

Neural recordings were performed on anaesthetized rats (1% Isoflurane, Isoba1 vet., Abbott Laboratories Ltd, Berkshire, England; n = 12). The recordings

commenced 1 day post implantation, and were performed approximately 1d/week for 8 weeks. During in vivo recordings (approximately 10 min/session), rats were connected to a Plexon data acquisition system (Plexon Inc, Texas, USA) via a head stage and pre-amplifier. Signals were band-pass filtered between 250 Hz to 8000 Hz. Recordings with estimated noise levels within 0.3 - 2 times the mean noise level across all recordings were included in the analysis. Putative single-unites were validated based on their mean-wave forms (polarity, shape, signal-to-noise ratio and amplitude) and firing statistics (percentage of inter-spike intervals shorter than 1 ms). Waveforms, which were not considered physiologically sound, or had an ISI-violation above 0.5% were rejected from the analysis.

**In-vivo impedance measurements and lesioning**

Impedance measurements: During the eight weeks period, in-vivo impedance at 1 kHz was measured once a week in four of the animals. To do that a Plexon stimulator 2.0 (Plexon Inc, Texas, USA) was used to generate a $\pm$ 100 nA 1 kHz sinusoidal current, and by monitoring the changes in voltage across the electrode, impedance was measured. It has been reported that the electrode impedance is influenced by the electrode-tissue interface properties, and that it is increased during elevated immune reactions. Thus, stable impedance values over time are indicating a stable electrode-tissue interface and/or limited immune response. As a final step, electrolytic lesion marks were produced by inducing sequentially 1 mA, 2 ms current through 6 wires/electrode bundle in deeply anaesthetized animal, using a DC-stimulator (Digitimer, Class I, model DS3, made in the UK). This was performed to confirm the probe location, and also to get more information regarding the in vivo wire spread within the rat brain. After this, animals were deeply anaesthetised and perfused and the brain was extracted for further histological evaluation.

# Statistical analysis (I, II, and IV)

For statistical analysis the Kruskal - Wallis test was performed, and Dunn's post hoc test was used to adjust for multiple comparisons. A p-value $< 0.05$ (*) was considered significant. All analyses were performed using the GraphPad Prism 6.0 software (GraphPad Software Inc., USA), (papers I, II, and IV). In studies I and II, all results presented in diagrams are depicted as box and whiskers diagrams indicating the median value. The box represents the 25th and 75th percentile and the whiskers represent the minimum and maximum values. In paper IV, the Mann - Whitney U-test was used for comparisons of the DRG tissue.

# Results and comments

## Effect of UVB irradiation on blood flow (I, II)

UVB irradiation of the glabrous skin on the rat hind paw induced an almost two-fold increase in skin blood flow on the irradiated side 24 h after UVB irradiation as compared to a naïve control group, which is in accordance with our previous findings (Ljunquist et al 2016). The skin blood flow on the contralateral side was not affected, i.e. measurements were almost identical for those obtained from the naïve animals. Increased skin blood flow is an inflammatory sign and blood flow increases have been observed in humans 12 h after UVB irradiation (Benrath et al 2001) and already after 2 h in rats (Eschenfelder et al 1995).

## Effect of UVB irradiation on DRG (I, II)

**Galanin**

In naïve control animals, about 10% of the neuronal profiles demonstrated galanin immunoreactivity, and these profiles could almost exclusively be classified as small-sized neurons. Previous reports have indicated that about 5% of the DRG neuronal population will show galanin immunoreactivity in the normal situation (Hökfelt et al 1987, Ji et al 1995, Shi et al 1999, Villar et al 1989). It is difficult to estimate what the proportion of galanin positive neurons should be, since galanin synthesis is a dynamic process which involves up to 40% of the DRG neurons under normal conditions (Lang et al 2015). After UVB irradiation the proportion of galanin immunoreactive neuronal profiles was reduced to 3.5% on the ipsilateral side and 5% on the contralateral side (Fig. 3 and 4). This reduction in the proportion of galanin positive DRG neurons occurred rapidly, already two hours after UVB irradiation. The findings of a reduced proportion of galanin positive DRG neurons after UVB induced inflammation are consistent with previous studies since galanin is usually down-regulated in DRG neurons after induced inflammation, but upregulated after nerve injuries (for review see Lang et al 2015).
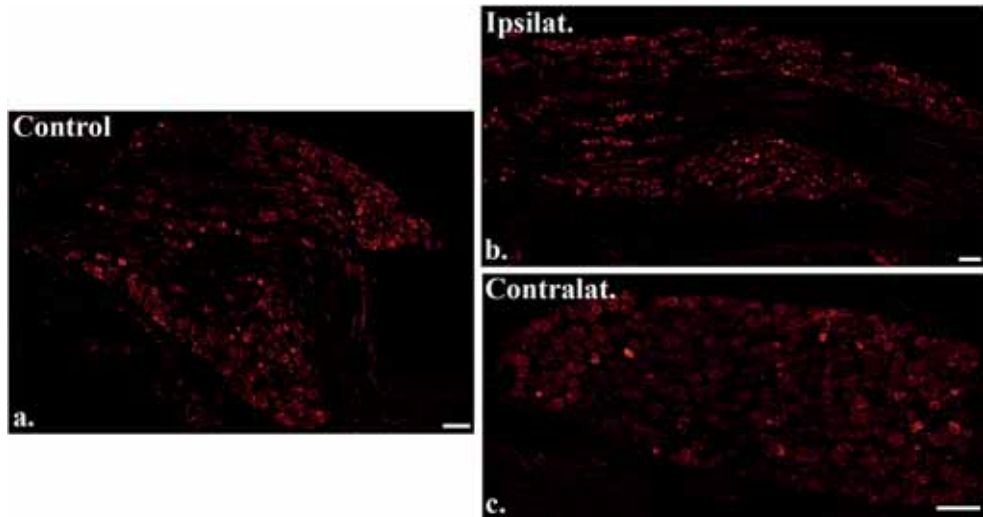
**Figure 3. Immunohistochemical staining of galanin positive neurons in ipsi- and contralateral DRG:L5 24 h after UVB irradiation.** The galanin positive neuronal staining (red) in the control group is depicted in (a). The proportion of galanin positive neurons had decreased 24 h (b and c) after UVB irradiation. Scale bar = 100 µm. Abbreviations: Ipsilat. = Ipsilateral side, and Contralat. = Contralateral side. Images (a and b) are reproduced from Etemadi L., Pettersson L.M., Danielsen N. UVB irradiation induces rapid changes in galanin, substance P and c-fos immunoreactivity in rat dorsal root ganglia and spinal cord. Peptides, 2017. 87: 71-83; open access publication.
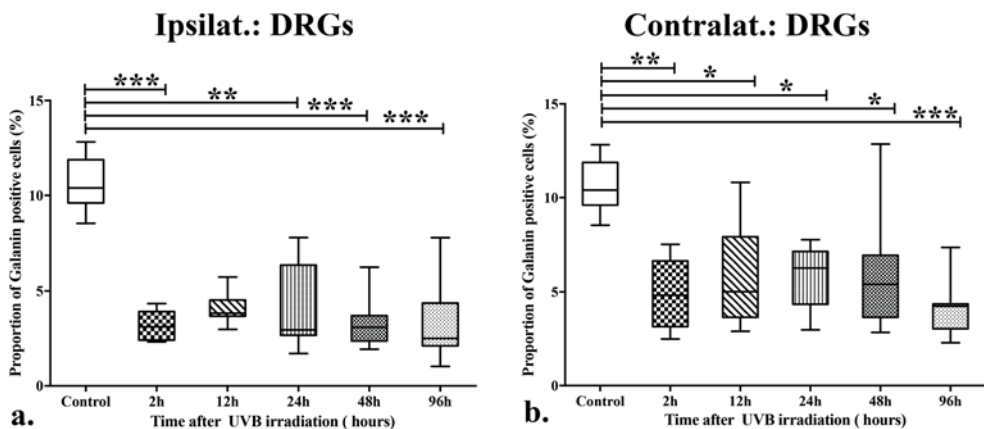


**Figure 4. Diagrams showing the proportion of galanin positive neurons in DRG:L5, ipsi- (a) and contralateral (b) to UVB irradiation.** In the control group the proportion of galanin positive neurons was about 10% of the counted population. After UVB irradiation the proportion was reduced to approximately 3.5% on the ipsilateral side and to 5% on the contralateral side at all time points examined. This decrease is statistically significant for all experimental groups except at 12 h (ipsilateral side), when compared to control DRGs (p < 0.001, n = 8 for all groups). Abbreviations: Ipsilat. = Ipsilateral side, and Contralat. = Contralateral side. Diagram (a) is reproduced from Etemadi L., Pettersson L.M., Danielsen N. UVB irradiation induces rapid changes in galanin, substance P and c-fos immunoreactivity in rat dorsal root ganglia and spinal cord. Peptides, 2017. 87: 71-83; open access publication.

## SP

In the control situation approximately 16% of the DRG neuronal profiles showed a positive immunoreactivity for SP. UVB irradiation did not induce any significant changes in this proportion on either ipsilateral- or contralateral sides. SP is one of the most common neuropeptides in DRG neurons and it has been reported that approximately 20% of the small DRG neurons contain SP (Hökfelt et al 1994) and inflammation will usually induce an increased synthesis of SP in DRG neurons (Noguchi et al 1988).

## C-fos

In the normal situation no c-fos expression could be detected in DRG neurons, an expected finding since c-fos expression is usually not described in DRG neurons. It was not possible to detect any induction of c-fos expression in DRG neurons on the inflamed side or on the contralateral side even if a specific anaesthetic regime was used that supposedly will not interfere with the c-fos expression.

# Effect of UVB irradiation on spinal cord (I, II)

## Galanin distribution

In the spinal cord, during normal conditions, galanin immunoreactivity could be detected in the superficial layers of the dorsal horn, as well as in the LSN area and in the area around the central canal (Fig. 5a). The galanin immunoreactivity was typically found in fibers. After UVB irradiation an increased immunoreactivity could be found in these areas on both the ipsi- and contralateral sides (Fig. 5b and c). On the ipsilateral side, significant changes were detected at 24 and 48 h after UVB irradiation for the dorsal horn + LSN area (Fig. 6a), at 12 and 24 h for the LSN area (Fig. 6c) and at 24, 48 and 96 h for the central canal area (data not shown here). In the LSN area, the galanin immunoreactivity was typically detected in nerve fibers (Fig. 7a). On the contralateral side, UVB irradiation also induced an increased galanin immunoreactivity in the dorsal horn + LSN area, in the LSN area alone, and in the area around the central canal. A significant increase in galanin immunoreactivity was detected 24 h after UVB irradiation for the contralateral dorsal horn + LSN area (Fig. 6b) and also for the LSN area alone (Fig. 6d). For the contralateral central canal area UVB irradiation induced a significant increase at all examined time points except at 96 h (data not shown here).
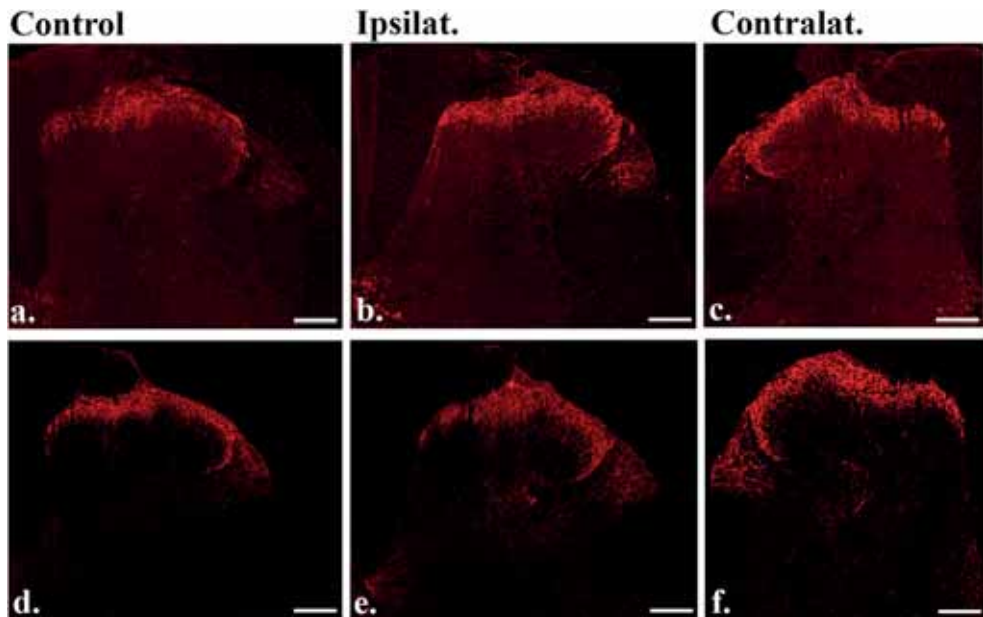
**Figure 5. Immunohistochemical staining of galanin (a, b and c ) and SP (c, d and f) in the L5 dorsal spinal cord area.** Spinal cord tissue from the control group is shown in (a), and (d). After UVB irradiation there was an increased immunopositive reactivity for galanin on both the ipsi- (b) and contralateral sides (c) 24 h after irradiation in the dorsal horn, in the area around the central canal and also the LSN area. The immunoreactivity for SP in the dorsal horn + LSN area was increased (48 h) after UVB irradiation on the ipsilateral side (e) and for the LSN area on the contralateral side (f). Scale bar = 200  µm. Abreviations: Ipsilat. = Ipsilateral side, and Contralat. = Contralateral side.

When comparing the ipsi- and contralateral sides, it seems that the induced changes are more obvious on the ipsilateral side as compared to the contralateral one (Fig. 6). As for the ipsilateral side the galanin immunoreactivity found in the LSN area was typically detected in fibers (Fig. 7b). For the central canal area (compare paper I and II), the magnitude for the induced changes in the proportion of galanin positive area is greater on the ipsilateral side.

An increase in immunoreactivity for galanin in the ipsilateral dorsal horn is not surprising, since previous reports have indicated that peripheral inflammation will induce an increased expression of galanin in the dorsal horn (for review see Liu and Hökfelt 2002). The finding of galanin immunoreactive fibers in the LSN area, on both the ipsi- and contralateral sides, after induced inflammation is more novel. Usually, the LSN area is not included in similar studies.
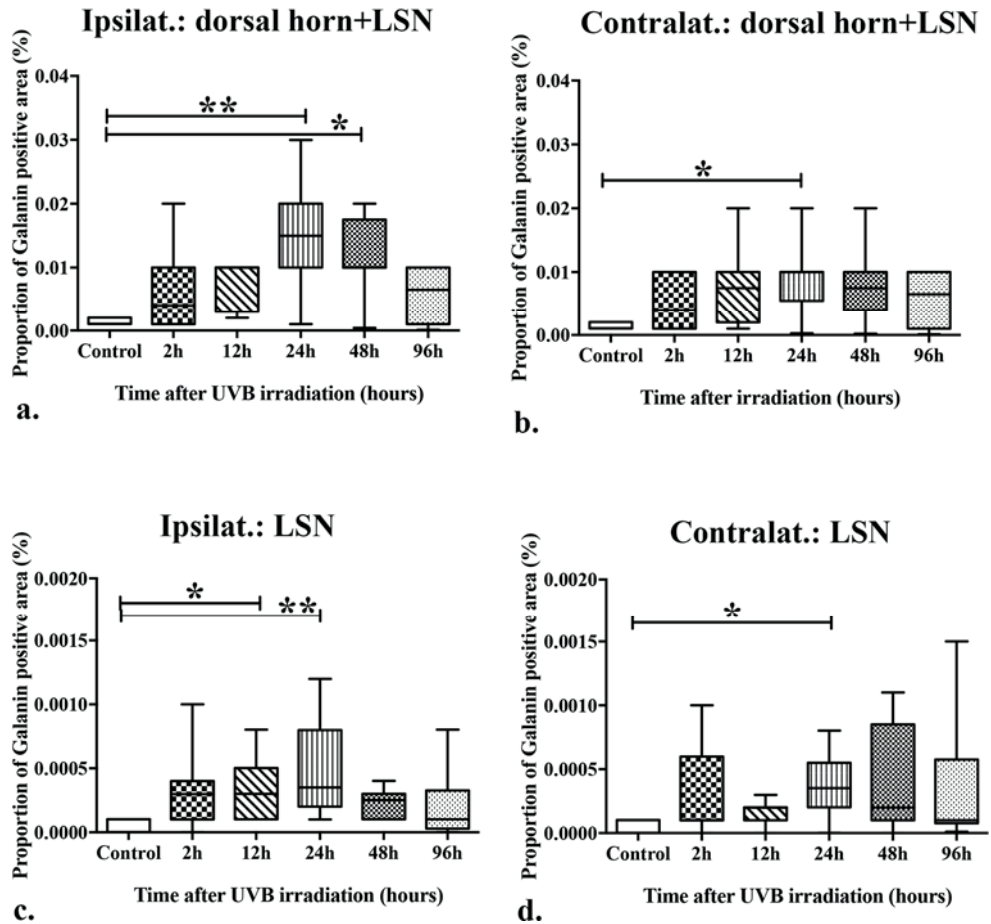
42

**Figure 6. Diagrams showing the proportion of galanin positive area in the L5 spinal cord dorsal horn and LSN area.** UVB irradiation caused an increased galanin immunoreactivity in the L5 dorsal horn + LSN spinal cord area on the ipsilateral side (a) and the contralateral side (b), as well as in the LSN area alone ipsi- and contralateral to UVB irradiation (c and d). The quantitative analysis showed that on the ipsilateral side the immunoreactivity for galanin (dorsal horn + LSN) was signficantly enhanced 24 and 48 h after UVB irradiation (a) as compared to control animals ($p < 0.05$; $p < 0.01$). Moreover, on the contralateral side a significant galanin increase was detectable 24 h after UVB exposure (b) as compared to control animals ($p < 0,05$). When the LSN area from both ipsi- (c) and contralateral sides (d) was quantified separately, the increased immunoreactivity was statistically significant 12 and 24 h after UVB irradiation on the ipsilateral side ($p < 0.05$; $p < 0.01$), and on the contralateral side it was only detectable 24 h after UVB irradiation ($p < 0,05$). Abbreviations: Ipsilat. = Ipsilateral side, and Contralat. = Contralateral side, LSN = lateral spinal nucleus.
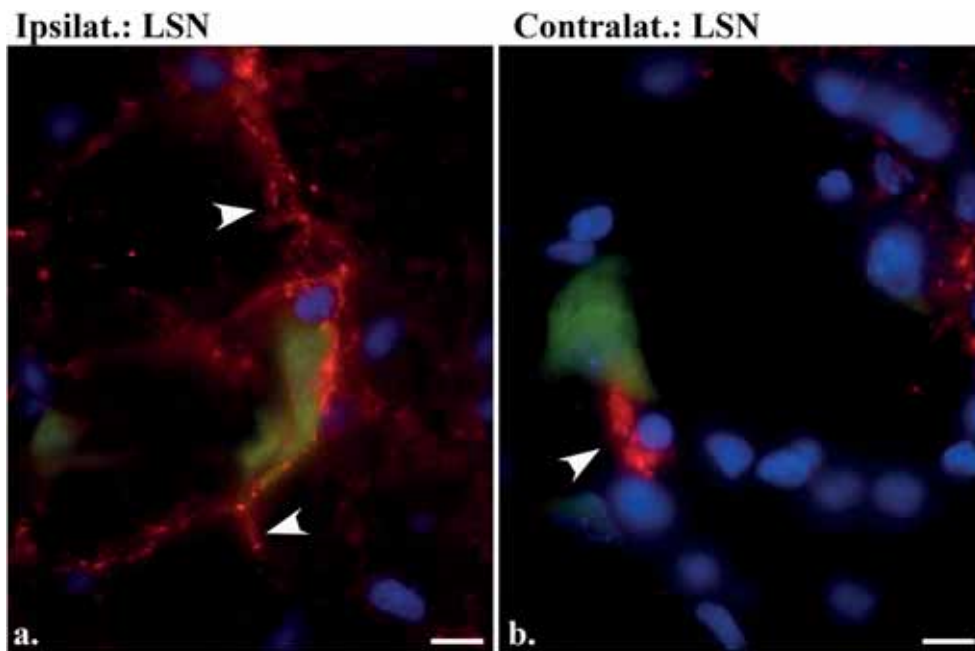
**Ipsilat.: LSN**  **Contralat.: LSN**

**Figure 7. Photomicrographs depicting galanin immunoreactivity (red), the neuronal marker HuC/HuD (green) and the nuclear marker DAPI (blue) in the LSN area of the L5 ipsi- (a) and contralateral (b) spinal cord dorsal horn 24 h after UVB irradiation.** Galanin immunoreactivity could be detected predominantly in fibers in the LSN area on both the ipsi- (a) and contralateral sides (b). Arrowheads are pointing at galanin positive fibers. Scale bar = 10 μm. Abbreviations: Ipsilat. = Ipsilateral side, and Contralat. = Contralateral side, LSN = lateral spinal nucleus.

## SP distribution

In the control group, SP immunoreactivity was mainly detected in the superficial layers in the dorsal horn, but also in the LSN area (Fig. 5d). In the LSN area the SP immunoreactivity was observable in nerve fibers. This finding correlates well to the observation made by Rea (2009), who reported presence of NK-1, one of the SP receptors, in the LSN area. After UVB irradiation the general impression was that of a slight increase of SP immunoreactivity in the dorsal horn area as well as in the LSN area for both the ipsi- and contralateral sides (Fig. 5 e and f). The increase for SP immunoreactivity in the superficial dorsal horn was less obvious than for galanin and had a larger variation. For both the ipsi- and contralateral sides the increased SP immunoreactivity in the LSN area was significant 48 h after UVB irradiation (Fig. 8).
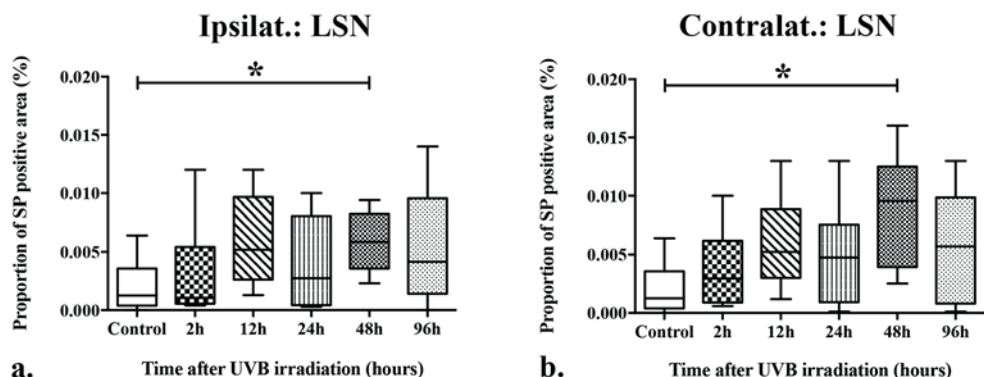
**Figure 8. Diagrams showing the proportion of SP positive area in LSN at the L5 spinal cord level. UVB irradiation induced an increased SP immunoreactivity in the LSN area of the L5 spinal cord.** On the ipsilateral side (a) a significant increase could be detected 48 h after UVB irradiation when compared to the control group (p < 0.05, separate Mann-Whitney U-test). Also on the contralateral side (b) a significant increase could be detected at the same time point after irradiation when compared to controls. Abbreviations: Ipsilat. = Ipsilateral side, and Contralat. = Contralateral side, LSN = lateral spinal nucleus.

## C-fos distribution

The qualitative analysis of c-fos immunoreactivity revealed that the dorsal horn area as well as the area around the central canal received a higher score for c-fos immunoreactivity 24 and 48 h after UVB irradiation on the ipsilateral side as compared to naïve controls. For the contralateral side a higher score was also obtained for the contralateral dorsal horn 24 and 48 h after UVB irradiation, whereas the data from scoring of the central canal area was similar but less obvious. It was not possible to detect c-fos immunoreactivity in the LSN area in naïve control animals or in any of the experimental groups. If c-fos immunoreactivity is a sign of an activated nervous system, the lack of c-fos activity in the LSN area supports the idea that the increase in galanin and SP immunoreactivity observed in this area are due to export/release of these neuropeptides from fibers innervating the LSN.

# Deep brain recording electrode (III)

## Electrode

The examination of the de-insulation procedure was performed using SEM, which confirmed the result of a clean metal surface. The decision was made to use a de-insulation length of 25 μm (± 5). Focused high intensity UV irradiation of the de-

insulated electrode tip caused transient boiling of the platinum and as a result an increase of the surface area was achieved along with a significant reduction in electrode impedance at 1 kHz (Mann-Whitney U-test).

## In vitro evaluation

One of the major goals of this study was to produce a flexible electrode with capacity to penetrate and spread out in deep targets in the brain. Therefore, an ultra-flexible platinum probe containing 29 ultrathin individual electrodes (28 recording electrodes) was developed and embedded in gelatine to ensure necessary mechanical stability allowing implantation. In order to reduce side effects, such as nerve tissue damage, caused by a too fast insertion velocity, it was necessary to increase the dissolution time for the gelatine vehicle. The electrodes embedded with gelatine in a single shank were therefore coated with Kollicoat™. The presence of a Kollicoat™ coating significantly increased the onset of dissolution time from $37 \pm 29$ sec to $114 \pm 75$ sec (Student t-test), when tested in a $37^{\circ}C$ agarose block.

In order to test if the increased dissolution time rendered by the Kollicoat™ was sufficient to maintain the integrity and mechanical stability of the gelatine embedded wire bundle (Fig. 9 and Fig. 10), further in vitro testing in agarose was performed. A pre-target depth of 7 mm was selected and the insertion speed was 100 µm/sec. When the pre-target depth was reached, a 10 min waiting pause was added allowing the gelatine to dissolve, and then the microelectrodes were inserted 1 mm deeper at a speed of 10 µm/sec. This procedure yielded a spread of $515 \pm 69$ µm (mean $\pm$ SD) in the agarose block, see Fig. 10.
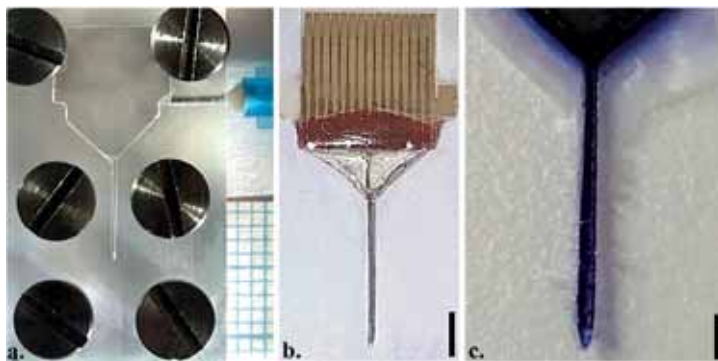


**Figure 9. Images visualizing the mould and probe after being embedded using the mould.** The manufactured mould (a) enabled gelatine embedding of the cluster electrode wires into a single shank (b) with a cone shaped tip (c) to facilitate the penetration during the implantation procedure. The kollicoated gelatine embedded electrode bundle had a diameter of ~250 µm). Scale bar: b = 2 mm, c = 1.25 mm. Picture (b) reproduced from Etemadi L., Mohammed M., Thorbergsson P.T., Ekstrand J., Friberg A., Granmo M., Pettersson L.M., Schouenborg J.Plos One 2016. 11(5): e0155109.; open access publication.
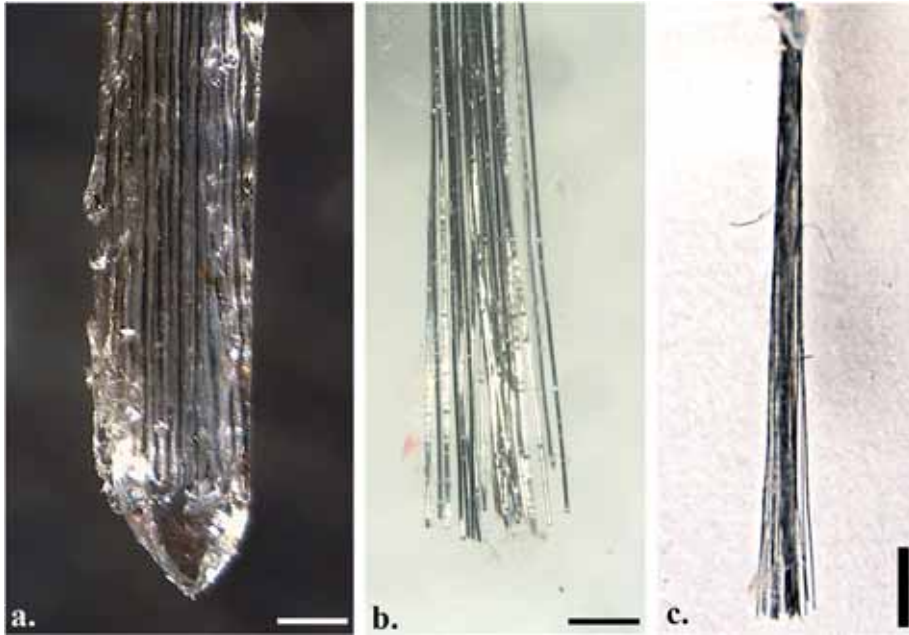
**Figure 10. Light field images depicting the kollicoated cluster electrode before and after in vitro experiments.** The kollicoated gelatine embedded electrode bundle (diameter ~250 µm) with a cone shaped tip before implantation (a). A close up of the probe visualizing the spreading (~500um) of the distal part of the probe into the 37°C agarose block (b). The straight implantation track of the electrode bundle inside the agarose is visualized in (c). Scale bar: a = 150 µm, b = 250 µm, and c = 1 mm. Picture reproduced from Etemadi L., Mohammed M., Thorbergsson P.T., Ekstrand J., Friberg A., Granmo M., Pettersson L.M., Schouenborg J.Plos One 2016. 11(5): e0155109.; open access publication.

## In vivo performance and histology

To evaluate the electrophysiological performance of the probe, after histological verification, eight animals in which the probe was targeting the intended subthalamic nucleus were selected. Statistical analysis showed that the percentage of functional channels remained stable over the experimental period (up to eight weeks; note that the recording started 1-2 days after implanting the probe). Moreover, it was noted that the median noise level increased gradually during the first four weeks. After this period no more significant changes were detected. The results of the histological verifications demonstrated that the probes maintained a straight track line and were placed correctly in the subthalamic nucleus in eight out of eleven rats. However, it should be pointed out that as the probes had spread out in the target zone some wires may have been located slightly anterior/posterior and/or medial or lateral to the target.

Electrically induced lesions were used to confirm separation of the individual electrode tips, and to verify the positioning within the subthalamic nucleus (Fig.

11). The average spread in vivo was $497 \pm 146$ µm, which is about the width of the rat subthalamic nucleus and also correlates well with the achieved in vitro spread ($515 \pm 69$ µm).
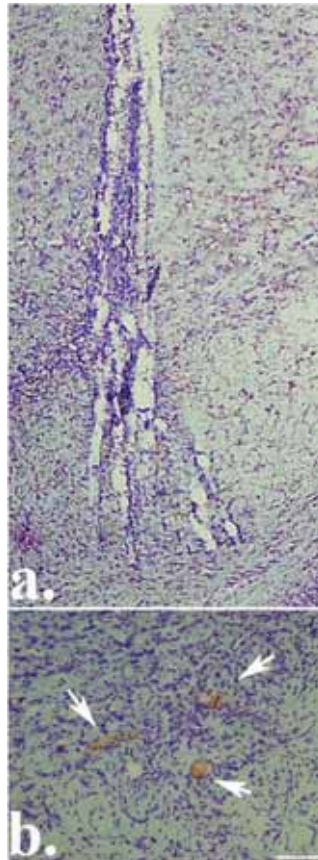


**Figure 11. Histological images visualizing the implantation track line and electrode spread in vivo.** Electrode implantation could be achieved through a narrow track line (a). Micrograph of electrically induced lesions in the subthalamic nucleus indicating electrode position (b). Cresyl violet staining was used to stain the brain sections for visualization of the probe track line and wire spread in the tissue. Scale bar: a = 100 µm, and b = 10 µm. Picture reproduced from Etemadi L., Mohammed M., Thorbergsson P.T., Ekstrand J., Friberg A., Granmo M., Pettersson L.M., Schouenborg J.Plos One 2016. 11(5): e0155109.; open access publication.

# Staining neurons using HuC/HuD and NeuN (IV)

## Qualitative analysis

When cortical sections stained with the HuC/HuD antibody were evaluated most of the staining protocols produced unacceptable quality (Fig. 12), an example is depicted in Fig. 13a (free floating sections with the antigen retrieval protocol, FHA). Free floating sections using the standard protocol for staining with HuC/HuD antibody (FHS) displayed the highest quality (Fig. 12 and 13b). For the other marker, NeuN, glass mounted sections using the standard protocol (GNS) gave the most unfavourable results (Fig. 13c), whereas if the antigen retrieval protocol was used images of good quality could be obtained for both free floating sections (Fig. 13d, FNA) and glass mounted sections (GNA).
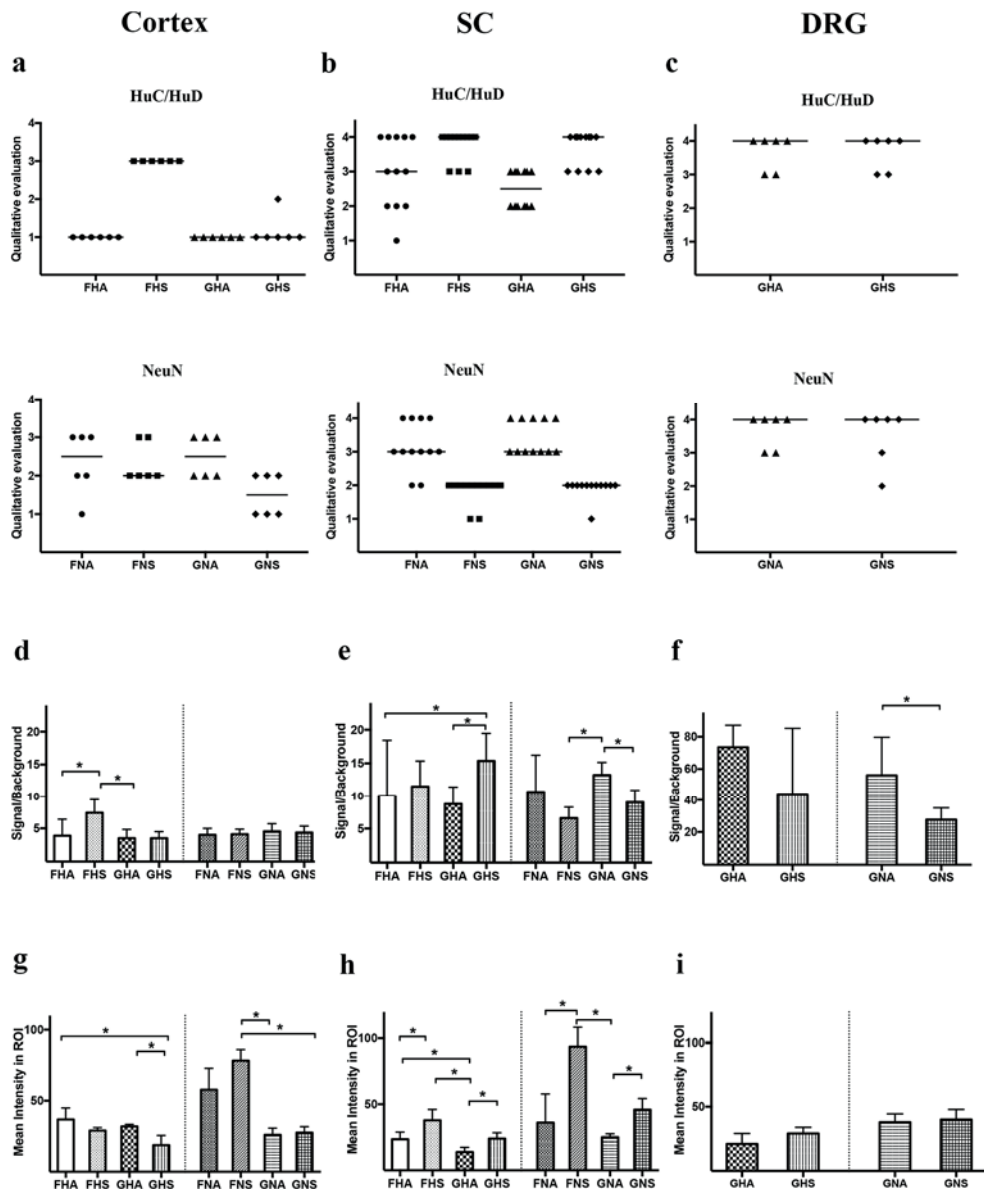
**Figure 12. Qualitative and quantitative evaluation of HuC/HuD and NeuN staining.** The results from the blind qualitative evaluation of HuC/HuD and NeuN staining of sections from cortex (a), spinal cord (SC) (b), and DRG (c) are depicted in the graphs, represented as scatterplots with indication of the median value. The signal/background analyses for cortex (d), SC (e) and DRG (f) are are also presented. In addition, the mean intensity of the immunohistochemical staining is evaluated in cortex (g), SC (h) and DRG (i). The bar graphs are indicating mean ± SD ($p < 0.05$, and n = 6).
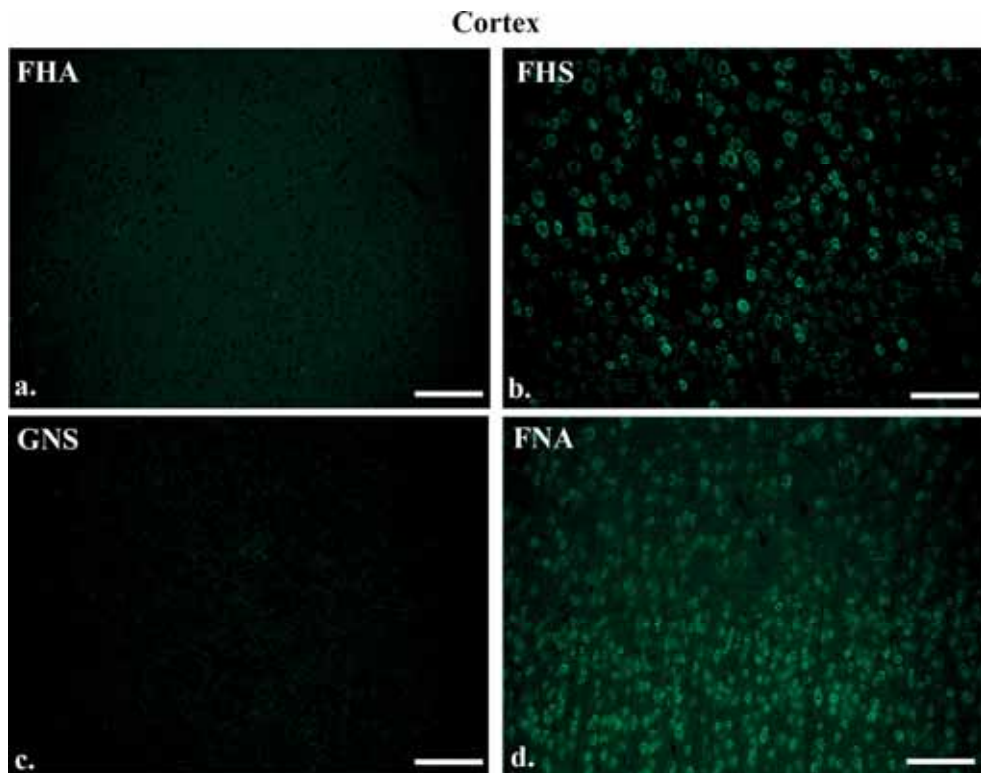
**Figure 13. Photomicrographs showing examples of brain cortical sections of unacceptable and good immunohistochemical quality.** The FHA treated sections (a) show an unacceptable quality, and the FHS treated sections (b) show the highest quality when staining for HuC/HuD in the cortex. For NeuN, GNS treated sections (c) show very poor tissue quality, and FNS treated sections (d) show the highest quality after immunostaining in the cortex. Scale bar = 100 µm, abbreviations: (FHA) free floating HuC/HuD antigen retrieval protocol, (FHS) free floating HuC/HuD standard protocol, (GNS) glass mounted NeuN standard protocol, and (FNA) free floating NeuN antigen retrieval protocol.

For the spinal cord tissue and the HuC/HuD antibody the antigen retrieval protocol (FHA and especially the glass mounted sections, GHA) produced the least favorable results (Fig. 12 (FHA and GHA) and Fig.14a GHA). If the standard protocol (FHS and GHS) was used, sections with high quality HuC/HuD staining could be obtained for either glass mounted or free floating sections (Fig. 14b, FHS). The NeuN antibody, did not work well if the standard protocol was applied on glass mounted (GNS) or free floating sections (Fig. 14c, FNS). For NeuN, acceptable results could be obtained if the antigen retrieval protocol was used for either free floating sections (FNA) or glass mounted sections (Fig. 14d, GNA).

To summarize, the antigen retrieval protocol is preferable in conjunction with NeuN staining, but for the HuC/HuD staining a standard protocol should be employed since the antigen retrieval protocol produced images of poor quality

when using this specific marker. It seems that the HuC/HuD antibody is giving better results than the NeuN antibody when staining spinal cord sections.

After examining the DRG images, it was found that staining with either of the antibodies yielded high quality images for glass mounted sections regardless of the type of staining protocol, standard or antigen retrieval (Fig. 14e and f).

## Signal/Background analysis

When staining cortex using the HuC/HuD antibody, the highest signal/background was obtained using the standard protocol for free-floating sections (FHS) (Fig 12d). This protocol also gave the best results in the qualitative analysis. FHS showed a statistically significant difference compared to the FHA and the GHA groups but not to GHS. After staining of cortex using the NeuN antibody, no significant differences were found when comparing the groups (Fig. 12d).

For spinal cord staining using the HuC/HuD antibody, the highest signal/background was obtained using the standard protocol for glass mounted sections (GHS), Fig. 12e. This protocol also gave very good qualitative results. GHS showed a statistically significant difference compared to the FHA and the GHA groups but not to the FHS group. Staining of the spinal cord using the NeuN antibody resulted in the highest signal/background when using the antigen retrieval protocol for glass mounted sections (GNA). This protocol gave on average acceptable qualitative results. GNA showed a statistically significant difference compared to the FNS and the GNS groups but not to FNA.

For the glass mounted DRGs stained with the HuC/HuD antibody, the highest signal/background was obtained using the antigen retrieval protocol (GHA), Fig. 12f. However, no statistically significant difference was found when comparing with the standard protocol (GHS) treated group. For glass mounted DRG sections stained with the NeuN antibody, the highest signal/background was obtained using the antigen retrieval protocol (GNA). GNA showed a statistically significant difference compared to the standard protocol GNS treated sections.

## Mean intensity evaluation

For cortex stained with the HuC/HuD antibody the highest mean intensity was obtained using the antigen retrieval protocol for free-floating sections (FHA), Fig. 12g. However, this protocol gave bad qualitative results. FHA showed a statistically significant difference compared to GHS. A statistically significant difference was also found when comparing GHA and GHS. For cortex stained with the NeuN antibody, the highest mean intensity was obtained using the

standard protocol for free-floating sections (FNS). However, this protocol gave lower qualitative scores. FNS showed a statistically significant difference compared to GNA and GNS.

For spinal cord stained with the HuC/HuD antibody the highest mean intensity was obtained using the standard protocol for free-floating sections (FHS), Fig. 12h. This protocol gave very good qualitative results. FHS showed a statistically significant difference compared to GHA and FHA groups. Statistically significant differences were also found when comparing GHS and GHA. For spinal cord stained with the NeuN antibody the highest mean intensity was obtained using the standard protocol for free-floating sections (FNS). However, this protocol gave poor qualitative results. FNS showed a statistically significant difference compared to FNA and GNA. A statistical significance was also found comparing GNS and GNA.

For DRG stained with the HuC/HuD antibody the highest mean intensity was obtained with the standard protocol (GHS) Fig. 12i. However, the difference was very slight and no statistically significant difference was found when comparing the two groups, GHS and GHA. For DRG stained with the NeuN antibody the highest mean intensity was also obtained using the standard protocol (GNS), but again the difference was very small and not statistically significant compared to the GNA group.
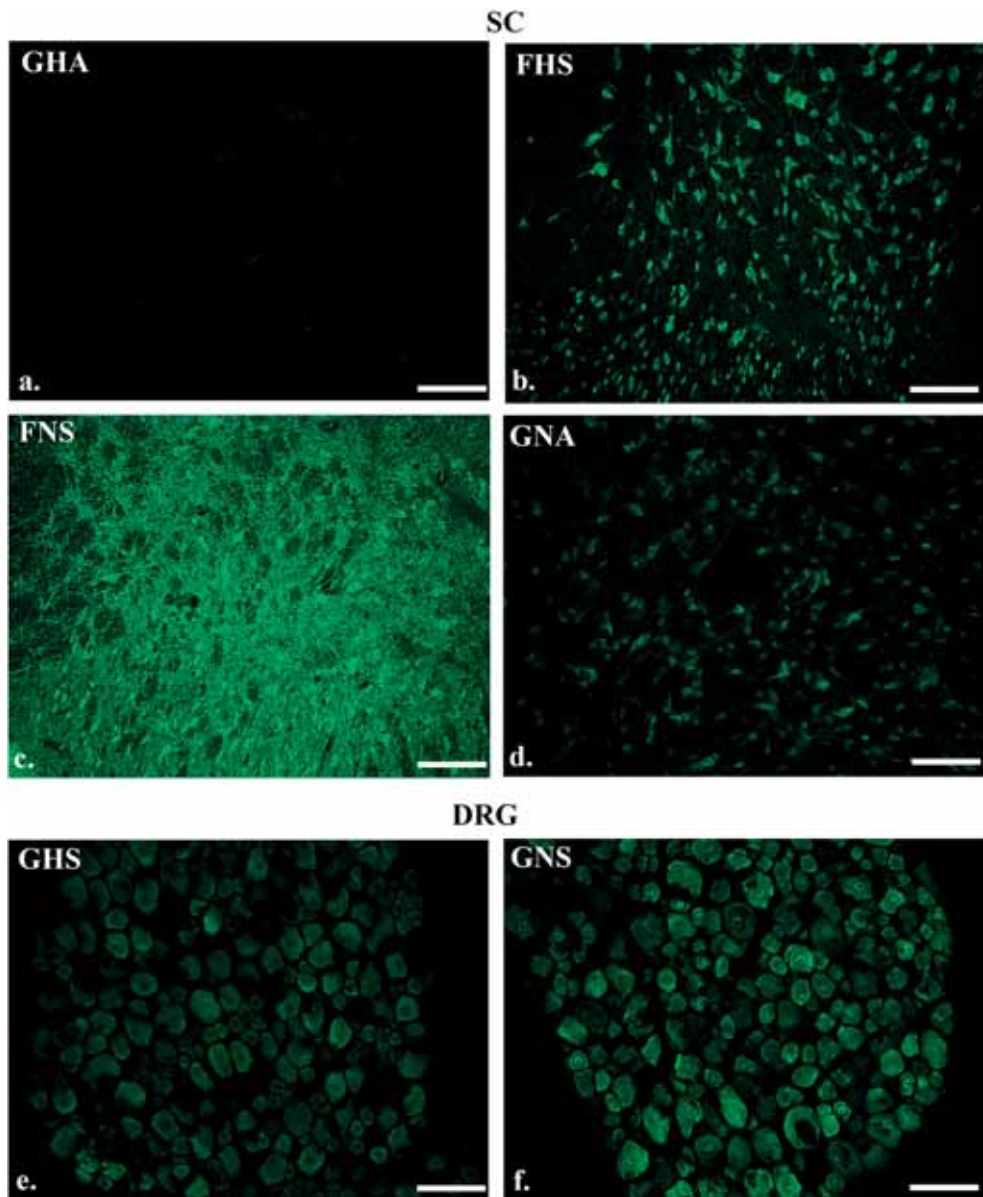
**Figure 14. Photomicrographs showing examples of spinal cord and DRG sections with unacceptable and good immunohistochemical quality.** The GHA (a) staining method yields unacceptable quality, and the FHS (b) represents the highest quality for HuC/HuD staining of the spinal cord dorsal horn. For NeuN staining, FNS (c) shows poor staining quality, and GNA (d) illustrates the highest staining quality for spinal cord dorsal horn. For DRG, very good quality of staining can be obtained using either HuC/HuD (e) or NeuN (f). Scale bar = 100 μm, abbreviations: (SC) spinal cord, (GHA) glass mounted HuC/HuD antigen retrieval protocol, (FHS) free floating HuC/HuD standard protocol, (GNA) glass mounted NeuN antigen retrieval protocol, (FNS) glass mounted NeuN standard protocol, (GHS) glass mounted HuC/HuD standard protocol, and (GNS) glass mounted NeuN standard protocol.

# General discussion

## The UVB model

UVB irradiation in a certain dose will induce inflammation, indicated by an increased blood flow as early as 12 h in humans (Benrath et al 2001) and already after 2 h in rats (Eschenfelder et al 1995). The findings presented in this thesis confirms that UVB irradiation induces an increased skin blood flow on the irradiated side, which was almost doubled as compared to the control situation (paper I). This result correlates well with another study using the same UVB irradiation paradigm (Ljungquist et al 2016). UVB irradiation will also induce other changes, such as a release of SP, which is involved in neurogenic inflammatory responses, and increasing vessel dilatation and permeability. The validity of the UVB irradiation model for studying inflammatory pain is supported by the fact that UVB irradiation of skin will induce inflammation and mechanical hyperalgesia in humans, rats and mice (Benrath et al 2001, Bishop et al 2007, Bishop et al 2009, Eschenfelder et al 1995, O´Neill et al 2015). Physiological studies have shown that UVB irradiation of human skin will induce hyperalgesic responses peaking after 24 - 32 h (Gustorff et al 2013), and a similar time window can be found in rats (Ljungquist et al 2016). In the rat study it was demonstrated that the recorded neuronal activity from the primary somatosensory cortex was significantly enhanced 24 h after UVB irradiation in response to both mechanical and thermal stimuli of the irradiated skin (referred to as primary hyperalgesia) and the adjacent area (referred to as secondary hyperalgesia. Evaluation of the UVB irradiation model suggests that it should be considered a translational pain model (Lopes and McMahon 2016). The model has advantages since it is non-invasive, and also the intensity of UVB irradiation can be varied.

# Inflammatory induced changes in the spinal cord, DRG and lateral spinal nucleus

The findings presented in this thesis indicate that unilateral UVB irradiation of the rat hind paw will induce biochemical changes in the lumbar segment of the spinal cord dorsal horn and corresponding DRGs, as well as around the central canal. These changes occur rapidly, on both the ipsi- and contralateral sides, within a time frame reported for the development of primary and secondary hyperalgesia. As indicators for biochemical alterations the neuropeptides galanin and SP were chosen. In addition induction of c-fos activity was evaluated. UVB irradiation induced a very rapid reduction of the proportion of galanin immunopositive neurons in both the ipsi- and contralateral DRGs, whereas the proportion of SP positive neurons did not change. The rapid reduction (already after 2 h and lasting for 96 h) suggests that galanin containing neurons on the ipsilateral side release/export their galanin content to the dorsal horn (Lang et al 2015) and the LSN area, and this hypothesis gains support from the observation of a corresponding increased immunoreactivity in these areas. It is well established that inflammation will induce a reduction of galanin positive DRG neurons and increase in galanin positive neurons in the dorsal horn (Ji et al 1995, Liu and Hökfelt 2002). The increased immunoreactivity for galanin in the dorsal horn may also be explained by an increased synthesis in spinal interneurons since galanin containing interneurons are present in lamina I and II (Lang et al 2015). The observed rapid change in the proportion of galanin positive DRG neurons gains support from other studies describing a rapid modulation of galanin in the lateral hypothalamic area already 4 h after peripheral inflammation (Lang and Kofler 2011, Sergeyev et al 2001), and in the lumbosacral DRGs after acute inflammation of the urinary tract (Girard et al 2008). The question is if the observed changes in galanin are related to nociceptive signalling and processing. The role of galanin in nociception is complex. It has been suggested that galanin has a dual role, being both pro- and antinociceptive during inflammation. Galanin is believed to initially facilitate pain transmission via DRG neurons and later block the signalling via dorsal horn neurons (Liu and Hökfelt 2002).

The changes in galanin observed on the ipsilateral side also occur on the contralateral side, but with a smaller magnitude. The contralateral DRG neurons probably also release/export galanin to the contralateral dorsal horn and LSN and the obvious question is how the contralateral DRG neurons can be affected by the peripheral inflammation. The underlying mechanism is unclear, but there are studies reporting similar phenomena. Inflammation on one side induces changes in neuropeptide levels in the contralateral DRG neurons (Mapp et al 1993, von Banchet et al 2000). For example, monoarticular arthritis induced bilateral

upregulation of NK-1 and bradykinin 2 receptors in rat DRG (von Banchet et al 2000) and it was suggested that the changes were due to a symmetrical afferent innervation of both sides of the spinal cord and that CNS contributes to bilateral inflammation and that efferent CNS activity might influence DRG neurons on both sides.

For the other neuropeptide studied, SP, there were no observable changes in the ipsi- or contralateral DRG neurons. In the dorsal horn, the changes were rather sparse and the only significant finding could be observed 48 h after UVB irradiation in the dorsal horn + LSN area on the ipsilateral side and in the LSN area only on the contralateral side. The changes in the ipsilateral dorsal horn + LSN area are probably due to changes in the LSN area alone, since significance could only be achieved when this area was tested alone. No such changes could be detected when the dorsal horn was tested alone.

An interesting finding in this thesis is the changes occurring in both the ipsi- and contralateral LSN after UVB irradiation of the skin. Changes in SP can be expected since this area contains NK-1, one of the receptors for SP (Rea 2009). Substance P is commonly detected in this part of the lumbar spinal cord (Leah et al 1988), and SP immunoreactive fibers and terminals can be detected in the lateral cervical nucleus in monkeys and rats (for review see Willis and Coggeshall 1991). In addition, LSN neurons have been shown to produce SP (Bresnahan et al 1984, Cliffer et al 1988) and the area also receives projections from SP containing spinal interneurons (Giesler and Elde 1985, Olave and Maxwell 2004). A possible explanation for the increased SP immunoreactivity in the LSN on both sides is the projections from primary afferents (Ling et al 2003, Rea 2009) activated by the UVB induced peripheral inflammation. The observation of galanin immuno-positive nerve fibers in the LSN and the bilateral inflammatory induced changes is more novel. The complexity of the projection patterns going to and from LSN, outlined in Figure 1, may explain the bilateral changes in neuropeptide content, both of SP and galanin, in this area. The primary afferents synapse directly or indirectly with LSN neurons on both sides, supporting the idea that changes occurring in DRG neurons on one side can affect the contralateral LSN area. Furthermore, the observed changes for galanin in the area around the central canal is not surprising. The central canal area receives nociceptive information from primary afferent fibers (Honda and Perl 1985, Nahin et al 1983, Rea 2009), and is thus also likely to be affected during the present conditions.


The role of LSN in nociceptive signalling is debated and complex. It seems that the cervical counterpart, the LCN, responds to noxious stimuli especially in cats and rats (Willis and Coggeshall 1991) and if this also applies to the LSN it is theoretically possible that the observed galanin immunopositive fibers may have a

role in nociceptive signalling in this part of the spinal cord. The rat LSN extend the entire length of the spinal cord and it has been suggested that this column is equal to the lateral cervical nucleus, but others have shown that rats have a specific LCN. The remaining column is the cervical part of the LSN (for review see Willis and Coggeshall 1991).

The observation of a bilaterally altered immunoreactivity for neuropeptides presumably involved in nociception, galanin and SP, as well as the presence of c-fos activity in areas related to nociceptive signalling, supports the claim that UVB induced inflammation will induce both primary and secondary hyperalgesia as observed and recorded in the rat somatosensory cortex by Ljungquist et al (2016).


# C-fos activity

Examination of c-fos activity in the nervous system is a rather common method for investigating the activity of the nervous system in pain research (Harris 1998). Peripheral painful stimulation usually induces the expression of this transcription factor in areas related to pain such as dorsal horn superficial layers, lamina V, and the area around the central canal. However, c-fos activation is not an exclusive sign of activation induced by noxious stimuli since induction of c-fos expression may occur in response to other stimuli as well (Harris 1998), thus questioning its value in pain research. The detection of c-fos expression is also affected by the anaesthetic regime used. It is recommended to use a mixture of fentanyl/ midazolam and to avoid using urethane since it promotes c-fos activation (Takayama et 1994). Others have reported that ketamine also influences c-fos immunoreactivity (Krukoff 1994). In paper I and II, the recommended mixture of fentanyl/midazolam was used. One might speculate that the use of this mixture made it possible to detect c-fos activity in the dorsal horn and in the area of the central canal 24 - 48 h after UVB irradiation without any further facilitating treatments. Previous studies have reported c-fos activity in these areas after UVB irradiation but only after an additional hot water bath treatment (Bishop et al 2007). The findings of c-fos immunoreactivity in the area around the central canal confirm the findings of Rea (2009) who reported that various noxious stimuli induced c-fos activity in this part of the nervous system. No c-fos activity could be detected in DRG neurons or in the LSN area. The lack of c-fos activity in DRG neurons is an expected finding considering previously published results, but since the specific anaesthetic regime was used in paper I and II it might give even firmer support to the conclusion that noxious stimuli do not induce c-fos activity in DRG neurons.

# Contralateral controls versus naïve controls

It is quite common to use the contralateral part of the nervous system as an inborn control when studying changes induced on the ipsilateral side after unilateral inflammation or nerve injury. However, there is a risk that the changes induced on the ipsilateral side are underestimated if the contralateral side is used as control. In the present work it was a deliberate choice to use naïve animals as controls (papers I and II). If the contralateral side would have been used as the control it may have not possible to detect the reduction in proportion of galanin immunopositive DRG neurons on the ipsilateral side. The ipsilateral proportion of galanin immuno-positive neurons was reduced to 3.5% compared to normal naïve rats where 10% of the DRG neurons expressed galanin. The corresponding number for the contralateral side was 5%. The difference between the ipsi- and contralateral sides was small and if the contralateral side would have been the control, the changes occurring on the ipsilateral side might have been undetected and indeed, an extended statistical analysis could not detect a difference between the ipsi- and the contralateral sides. The use of naïve intact animals as the controls is also crucial when studying areas within the nervous system that have projections across the midline, e.g. the LSN (Olave and Maxvell 2004, Petko and Antel 2000, Rea 2009).

The use of the contralateral side as the control is questionable. It is recommended that naïve intact animals are used as controls in order to detect changes occurring on the ipsilateral side. The contralateral side should probably be tested against naïve intact animals in order to detect if changes will be induced also on this side.

# Development of a new generation of electrodes

The purpose of the development and manufacturing of an implantable mechanically flexible electrode construct was to enable targeting of deeper brain structures more precisely and also to be able to target several neurons within these deeper brain structures by spreading of the different individual electrode wires. The approach chosen was intended to overcome some of the existing issues related to stability of recordings, implantation of flexible probes, precise targeting of deeper structures and high spatial resolution of the recordings. In order to reach a larger number of neurons, within a target nucleus, a multi-wire design was chosen, where the individual electrodes consisted of ultrathin platinum wires. Moreover, a specific tailor made mould was constructed to ensure the alignment of the probe shank. This mould could also be used to gather and embed the individual wires into a solitary shank with sharp tip using gelatine. Implantation of a flexible construct into the brain requires some sort of mechanical stability during the

implantation procedure, either e.g. by a rigid guide which is later removed or as in this thesis, by embedding the electrodes in a gelatine matrix which later dissolves. Gelatine has the advantage that it will give a flexible construct mechanical stability, thus allowing implantation into the brain. Gelatine will dissolve when in contact with liquids, i.e. after insertion into the brain. In addition, gelatine will likely also reduce the intensity of the elicited tissue reaction (Lind et al 2010). In order to prevent dissolution of the gelatine matrix during insertion into deep brain areas, one alternative would be to increase the implantation velocity. However, it is known that high-speed probe insertions will damage brain tissue and destroy blood vessels (Johnson et al 2007). To avoid having to increase the insertion speed it was necessary to increase the gelatine dissolution time to maintain the mechanical support afforded by the gelatine matrix. This was achieved by coating the gelatine with Kollicoat™, which significantly increased the onset of dissolution of the gelatine matrix.

A number of adjustments and control experiments were made in vitro to define all necessary parameters (see paper III) before implanting these multi-array electrodes in vivo. Paper III demonstrates that the designed electrode construct, together with a meticulous implantation procedure, could be used to reach deeper brain structures and that these electrodes are functional as demonstrated by long-term recordings (eight weeks) from awake, freely moving animals. One of the disadvantages of current deep electrodes is that their functions deteriorate, or is even lost over time. This is partly due to the elicited tissue reactions, such as glial scarring (Nolta et al 2015), triggered by the implantation itself as well as the inserted constructs. The obtained recordings from this new generation of electrodes showed significant stability of the impedance and signal to noise ratio over a time period of eight weeks.

The design of the present electrode construct can be modified for targeting other deep brain structures known to be involved in nociceptive signalling, e.g. thalamus or the periaqeuductal grey (PAG). PAG is known to influence nociceptive signalling (Loyd and Murphy 2009), but its location in the brain stem makes it more difficult to target. The constructed electrode device could, after modifications, be implanted in deeper brain structures for recording signals received from a peripheral inflamed area, and at the same time record and correlate with signal input to the somatosensory cortex (Ljungquist et al 2016), or by turning the device into a stimulatory one, and thus combine deep brain stimulation with an analysis on its effects on signals recorded from the somato-sensory cortex. Adjustments of the electrode construct can be made by e.g. changing the length of the individual electrodes and also adjustment of the spreading pattern.

# Staining neurons

The individual papers in this thesis rely on proper identification of neurons. In the two first papers neuron identification was used to define the proportion of DRG neurons containing the two different neuropeptides investigated and how these proportions changed after peripheral inflammation. The anti-HuC/HuD antibody was used to detect neurons in DRG and spinal cord and the comparison between this antibody and another neural marker, the anti-NeuN antibody, favoured the anti-HuC/HuD antibody as demonstrated in paper IV. In addition, our laboratory regularly use anti-NeuN antibody when visualizing neurons in cortical sections, in some cases in conjunction with an antigen retrieval protocol (Gällentoft et al 2015). The question is if the two antibodies will function in all situations. There are indications that the anti-NeuN antibody is not performing well on spinal cord sections from aging rats (Portiansky et al 2006) or on striatal sections from old rats when compared with sections from cortex or hippocampus (Gällentoft et al 2012). It is generally assumed that these pan-neuronal markers also function well for staining tissue after injury, e.g. implantation of recording electrodes, and they probably will since both the anti-NeuN antibody (Mullen et al 1992) and the anti-HuC/HuD antibody (Marusich et al 1994) label neurons after they left the mitotic cycle. Implantation of electrodes will cause tissue damage provoking astrocytic reactions but this damage and reactions can be substantially reduced if the correct procedures and constructs are used (Köhler et al 2015, Lind et al 2010). However, in order to evaluate the histological basis and confirm the feasibility of long term neurophysiological recordings, it is necessary to verify that neurons are in close vicinity to the electrodes, thus a reliable neuronal marker is of essence.

The signal/background ratio quantifications can be used as an indicator of the quality of the histological image together with the more obvious qualitative evaluation of the sections. In another biomedical field, bacteriology, it has been suggested that signal-to-noise measurements can be used for eliminating weakly fluorescent structures and artifacts but also for evaluating the image and its quality (Danielsen and Nordenfeldt 2017). Computer vision-based image analyses rely on automation, completeness and access to invisible data whereas human vision rely on the association of the observed image with previous experiences. Human vision analysis has a disadvantage since it may be incomplete and that it may vary between individuals, but since the human memory for images is large the association strategy used by humans allows for rapid interpretation of weakly defined images (Danuser 2011). The methods in paper IV can be used for evaluating the quality of immunohistochemical staining, but for quantification other methods have to be applied as out lined in paper I and II.

# Conclusions

- UVB irradiation of rat skin induces rapid biochemical changes, as indicated by the observed changes for galanin, substance P and c-fos, in the sensory part of the nervous system.

- The observed changes for galanin and substance P occur within a corresponding time frame as the neurophysiological changes detected in rats and humans after UVB irradiation.

- Unilateral UVB irradiation will induce increased immunoreactivity for galanin and substance P in the lateral spinal nucleus on both sides of the spinal cord. The findings observed for galanin can be considered novel.

- The changes observed for galanin, substance P and c-fos occur on both the ipsi- and contralateral sides of the spinal cord after unilateral UVB induced inflammation, which indicates that the contralateral side should not be used as the control.

- A new generation of mechanically flexible, multichannel electrode has been constructed that can be used to record neurophysiological signals from deep brain structures in awake, freely moving rats for a relative long period of time.

- Different antibodies used to visualize neurons will give results of varying quality, depending on which part of the nervous system is analysed and what staining protocol is used. For spinal cord and cortical sections the anti-HuC/HuD antibody gave the most favourable results. However, for cortex, the anti-NeuN antibody in conjunction with an antigen retrieval protocol gave similar results.

# Acknowledgements

First, I would like to express my gratitude to,

**Professor Nils Danielsen**, my supervisor, for always welcoming me to discuss my questions no matter what time of the day. Your fantastic patience and guidance throughout the work, and your great attitude making a scientific project moving forward has always been inspiring. Also, I am really thankful for all of those *Italian dinners! *, as you have called them.

**Professor Jens Schouenborg**, head of the Neuronano Research Center, thanks for giving me the great opportunity to pursue my Ph.D., your patience and never-ending reflection on scientific issues is really instructive.

**Dr. Lina Pettersson**, a Big Thanks for all your uniquely detailed comments, you always make me wonder about your special talent to see so many different angles in a scientific discussion, your great effort for understanding the true meaning of the scientific concept is truly inspiring.

Also,

Special thanks to **Lars-Åke Clementz**, whose intelligent ideas and endless enthusiasm for designing new technical equipment had a great influence on my work, your memory is always in my heart!

My great appreciation to: Suzanne Rosander-Jönsson, for your professional laboratory skills and being the only one who could support a day full of action in the lab very calmly, Peter Paulander for all early morning engineering support and consulting, Petter Pettersson for interesting electronic discussions specially for understanding the complications of the Gamry system, Agnetha SanMartin for valuable advice and unique encouragement to try the newest techniques in the lab, Andrea Nord and Linda Eliasson for all great support and letting me know, that you always are there whenever I need you.

Warm thanks to all the people in the lab, and also my fellow PhD students, past and present, who made a day in NRC, an informative day: Martin Garwicz, Per Petersson, Cecilia Eriksson, Jonas Thelin, Mengliang Zhang, Annika Friberg, Lucas Kumosa, Palmi Thor Thorbergsson, Ulrike Richter, Pär Halje, Niclas Lindqvist, Ali Ghasemi Azar, Per Köhler, Veronica Johansson, Bengt Ljungquist, Tanja Jensen, Gustav Lind, Martin Tamté, Lina Gällentoft, Mohsin Alexander Holmkvist, Johan Agorelius.

With a special thanks to Nela Ivica and Matilde Forni, teaching vestibularis lab was such a great experience and fun with you two dear friends. Thanks for all fantastic talks, inspiration and encouragement. I wish both of you enthusiastic

researchers, great luck and success during your PhD education and also for your future career.

Also, I dearly would like to thank my fantastic friends who have been supportive by their wise and kind words along the way:

Ingegerd Wirtberg and Ingrid Johansson, I am so proud knowing such successful experts and strong ladies, your professional advice was a rescue rope when I was at the bottom of the hole!

Britta and Olle Hammar, my warm and reliable friends, who are endlessly enjoying scientific and cultural discussions over a delicious supper, you make one feel that life is full of positive things, and of course problems exist, but in nano-scales!

Anna and Bengt Rippe, it is not an every day life opportunity to get a chance to know people like you! Even though the loss of precious Bengt, such an unique human and genius, is indeed a tremendous loss, I still feel so lucky for having you, my fantastic Anna.

Lisette Eklund, Eva Hallgren, Jolanda Witteveen, the lovely Italian couple Irene Sebastianutto and Francesco Bez, Pawel Markowicz, for all of your smart tips and happy times we had together, and still more to come!

**To my dearest family**, it is not easy at all to put it all into words. I just would like you to know that I am wholeheartedly thankful to all of you, without you I could not see myself on a fantastic road, pursuing wonders of neuroscience as I have always wished: My father Mahmoud Etemadi, Kerstin Nyström, Bahare and Bahram Etemadi, Farideh Etemadi and Mahmoud Zarrinnam.

And at last but not least, this work is for you **Martin Nyström**, for being You, and The Most Special to Me! I am not quite sure that you are going to read this book ever, as it unfortunately contains nothing about V8 engines, but *by all means, it is yours*!, and I can promise you, over these years, all those afternoons standing by your side with my special mechanical gloves, watching curiously your inexhaustible, unbeatable, and enthusiast works on different engines and all those lovely delicate cookies made by You, had so much to do with it until this End! ☺

# References

Alivisatos A.P., Chun M., Church G.M., Greenspan R.J., Roukes M.L., Yuste R. The Brain Activity Map Project and the Challenge of Functional Connectomics. *Neuron.* 2012;74(6):970-974.

Alvarez F.J., Villalba R.M., Carr P.A., Grandes P., Somohano P.M. Differential distribution of metabotropic glutamate receptors 1a, 1b and 5 in the rat spinal cord. *J Comp Neurol.* 2000;422(3):464-487.

Alvarez F.J., Villalba R.M., Zerda R., Schneider S.P. Vesicular glutamate transporters in the spinal cord, with special reference to sensory primary afferent synapses. *J Comp Neurol.* 2004;472(3):257-280.

Benabid A.L., Pollak P., Gao D., Hoffmann D., Limousin P., Gay E., Payen I., Benazzouz A. Chronic electrical stimulation of the ventralis intermedius nucleus of the thalamus as a treatment of movement disorders. *J Neurosurg.* 1996;84(7):203-214.

Benrath J., Gillardon F., Zimmermann M. Differential time courses of skin blood flow and hyperalgesia in the human sunburn reaction following ultraviolet irradiation of the skin. *Eur J Pain.* 2001;5(2):155-167.

Berthoud H.R., Patterson L.M., Willing A.E., Mueller K., Neuhuber W.L. Capsaicin-resistant vagal afferent fibers in the rat gastrointestinal tract: anatomical identification and functional integrity. *Brain Res.* 1997;746(1-2):195-206.

Bishop T. ,Marchand F., Young A.R., Lewin G.R., McMahon S.B. Ultraviolet-B-induced mechanical hyperalgesia: A role for peripheral sensitisation. *Pain.* 2010;150(1):141-152.

Bishop T., Ballard A., Holmes H., Young A.R., McMahon S.B. Ultraviolet-B induced inflammation of human skin: characterisation and comparison with traditional models of hyperalgesia. *Eur J Pain.* 2009;13(5):524-532.

Bishop T., Hewson D.W., Yip P.K., Fahey M.S., Dawbarn D., Young A.R., McMahon S.B. Characterisation of ultraviolet-B-induced inflammation as a model of hyperalgesia in the rat. *Pain.* 2007;131(1-2):70-82.

Bresnahan J.C., Ho R.H., Beattie M.S. A comparison of the ultrastructure of substance-P and enkephalin immunoreactive elements in the nucleus of the dorsal lateral funiculus and laminae I and II of the rat spinal cord. *J Comp Neurol.* 1984;229(4):497-511.

Buston C.R., McIntyre C.C. Role of electrode design on the volume of tissue activated during deep brain stimulation. *Neural engineering.* 2006;3:1-8.

Buzsáki G. Large-scale recording of neuronal ensembles. *Nat Neurosci.* 2004;7(5):446-451.

Carniglia L., Ramírez D., Durand D., Saba J., Turati J., Caruso C., Scimonelli T.N., Lasaga M. Neuropeptides and Microglial Activation in Inflammation, Pain, and Neurodegenerative Diseases. *Mediators Inflamm.* 2017;2017:23 pages.

Chung K., Lee W.T., Carlton S.M. The effects of dorsal rhizotomy and spinal cord isolation on calcitonin gene-related peptide-labelled terminals in the rat lumbar dorsal horn. *Neurosci Lett.* 1988;90(1-2):27-32.

Cliffer K.D., Urca G., Elde R.P., Giesler G.J. Jr. Studies of peptidergic input to the lateral spinal nucleus. *Brain Res.* 1988;460(2):356-360.

Coons A.H., Creech H.J., Jones R.N. Immunological properties of an antibody containing a fluorescent group. *Proc Soc Exp Biol Med.* 1941;47:200-202.

Craig A.D. Pain mechanisms: labeled lines versus convergence in central processing. *Annu Rev Neurosci.* 2003;26:1-30.

Craig A.D., Dostrovsky J.O. Thermoreceptive lamina I trigeminothalamic neurons project to the nucleus submedius in the cat. *Exp Brain Res* 1991;85(2):470-474.

Dagci T., Armagan G., Konyalioglu S., Yalcin A. Alterations in the expression of the apurinic/apyrimidinic endonuclease-1/redox factor-1 (APE/ref-1) and DNA damage in the caudal region of acute and chronic spinal cord injured rats treated by embryonic neural stem cells. *Physiol Res* 2009;58(3):427-434.

Dalmau J., Furneaux H.M., Gralla R.J., Kris M.G., Posner J.B. Detection of the anti-Hu antibody in the serum of patients with small cell lung cancer--a quantitative western blot analysis. *Ann Neurol.* 1990;27(5):544- 552.

Danielsen J., Nordenfelt P. Computer Vision-Based Image Analysis of Bacteria. In Bacterial Pathogenesis: Methods and Protocols (Pontus Nordenfelt and Mattias Collin eds). *Methods Mol Biol* 2017;1535:161-172, doi: 10.1007/978-1-4939-6673-8_10. ©Springer Science + Business Media, New York 2017.

Danuser G. Computer Vision in Cell Biology. *Cell.* 2011;147:973-978.

Das V. An introduction to pain pathways and pain "targets". *Prog Mol Biol Transl Sci.* 2015;131:1-30.

Denny-Brown D. Primary sensory neuropathy with muscular changes associated with carcinoma. *J Neurol Neurosurg Psychiatry.* 1948;11(2):73-87.

Di Giminiani P., Petersen L.J., Herskin M.S. Characterization of nociceptive behavioural responses in the awake pig following UV-B-induced inflammation. *Eur J Pain.* 2014;18(1):20-28.

Dray A. Inflammatory mediators of pain. *Br J Anaesth.* 1995;75(2):125-131.

Du J., Riedel-Kruse I.H., Nawroth J.C., Roukes M.L., Laurent G., Masmanidis S.C. High-resolution three-dimensional extracellular recording of neuronal activity with microfabricated electrode arrays. *J Neurophysiol.* 2009;101(3):1671-1678.

Dubuisson D., Dennis SG. The formalin test: a quantitative study of the analgesic effects of morphine, meperidine and brain stem stimulation in rats and cats. *Pain.* 1977;4(2):161-174.

Eschenfelder C.C., Benrath J., Zimmermann M., Gillardon F. Involvement of substance P in ultraviolet irradiation-induced inflammation in rat skin. *Eur J Neurosci.* 1995;7(7):1520-1526.

Gabriëls L., Cosyns P., Nuttin B., Demeulemeester H., Gybels J. Deep brain stimulation for treatment-refractory obsessive-compulsive disorder: psychopathological and neuropsychological outcome in three cases. *Acta Psychiatr Scand.* 2003;107(4):275-282.

Gibson S.J., Polak J.M., Bloom S.R., Wall P.D. The distribution of nine peptides in rat spinal cord with special emphasis on the substantioa gelaitnsa and in the area around the central canal (lamina X). *J Comp Neurol.* 1981;201(1):65-79.

Giesler Jr G.J., Elde R.P. lmmunocytochemical studies of the peptidergic content of fibers and terminals within the lateral spinal and lateral cervical nuclei. *J Neurosci.* 1985;5(7):1833-1841.

Girard B.M., Wolf-Johnston A., Braas K.M., Birder L.A., May V., Vizzard M.A. PACAP-Mediated ATP release from rat urothelium and regulation of PACAP/VIP and receptor mRNA in micturition pathways after cyclophosphamide (CYP)-induced cystitis. *J Mol Neurosci.* 2008;36(1-3):310-320.

Giuffrida R., Rustioni A. Dorsal root ganglion neurons projecting to the dorsal column nuclei of rats. *J Comp Neurol.* 1992;316(2):206-220.

Grubb B.D., Stiller R.U., Schaible H.G. Dynamic changes in the receptive field properties of spinal cord neurons with ankle input in rats with chronic unilateral inflammation in the ankle region. *Exp Brain Res.* 1993;92(3):441-452.

Grudt T.J., Perl E.R. Correlations between neuronal morphology and electrophysiological features in the rodent superficial dorsal horn. *J Physiol.* 2002;540(Pt 1):189- 207.

Gundlach A.L. Galanin/GALP and galanin receptors: role in central control of feeding, body weight/obesity and reproduction? *Eur J Pharmacol.* 2002;440(2-3):255-268.

Gusel'nikova V.V., Korzhevskiy D.E. NeuN As a Neuronal Nuclear Antigen and Neuron Differentiation Marker. *Acta Naturea.* 2015;7(2):42-47.

Gustorff B., Sycha T., Lieba-Samal D., Rolke R., Treede R.D., Magerl W. The pattern and time course of somatosensory changes in the human UVB sunburn model reveal the presence of peripheral and central sensitization. *Pain.* 2013;154(4):586-597.

Gwyn D.G., Waldron H.A. A nucleus in the dorsal lateral funiculus of the spinal cord of the rat. *Brain Res.* 1968;10(3):342-351.

Gällentoft L. Pettersson L.M., Danielsen N., Schouenborg J., Prinz C.N., Linsmeier C.E. Size-dependent long-term tissue response to biostable nanowires in the brain. *Biomaterials.* 2015;42:172-183.

Gällentoft LE, Lind G, Trobäck A, Pettersson LME, Eriksson Linsmeier C. Age-related changes of Neuronal Nuclei (NeuN) expression in different areas of the rat brain. 42nd Annual Meeting Society for Neuroscience, New Orleans, LA; USA, October 13-17, 2012. Program No. 87.08 Abstract viewer/itinerary planner. Washington, DC: Society for Neuroscience, 2012. Online.

Harris J.A. Review: Using c-fos as a Neural Marker of Pain. *Brain Res Bull.* 1998;45(1):1-8.

Herrero J.F., Laird J.M., López-García J.A. Wind-up of spinal cord neurones and pain sensation: much ado about something? *Prog Neurobiol.* 2000;61(2):169-203.
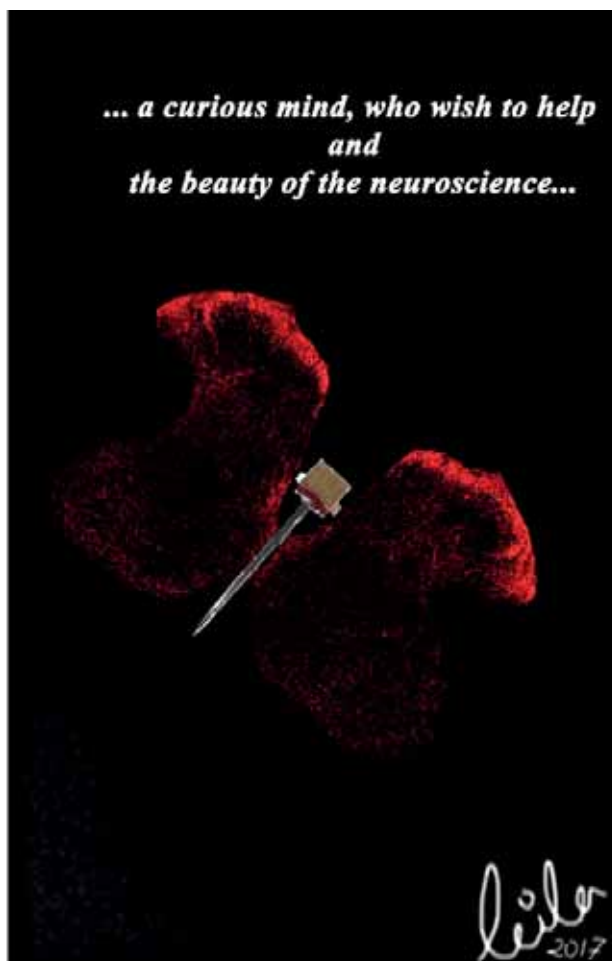
Hodaie M., Wennberg R.A., Dostrovsky J.O., Lozano A.M. Chronic anterior thalamus stimulation for intractable epilepsy. *Epilepsia.* 2002;43(6):603-608.

Honda C.N., Perl E.R. Functional and morphological features of neurons in the midline region of the caudal spinal cord of the cat. *Brain Res.* 1985;340(2):285-295.

Hunt S.P., Pini, A., Evan, G. Induction of c-fos-like protein in spinal cord neurons following sensory stimulation. *Nature.* 1987;328:632-634.

Hökfelt, T., Wiesenfeld-Hallin,Z., Villar,M., Melander,T. Increase of galanin-like immunoreactivity in rat dorsal root ganglion cells after peripheral axotomy. *Neuroscie Lett.* 1987;83(3):217-220.

Hökfelt T., Zhang X., Wiesenfeld-Hallin Z. Messenger plasticity in primary sensory neurons following axotomy and its functional implications. *Trend Neurosci.* 1994;17(1):22-30.

International Association for the Study of Pain. IASP Taxonomy. *http://www.iasp-pain.org/Education/Content.aspx?ItemNumber=1698&navItemNumber=576*

Jansen A.S., Loewy A.D. Neurons lying in the white matter of the upper cervical spinal cord project to the intermediolateral cell column. *Neuroscience.* 1997;77(3):889-898.

Ji R.R., Zhang X., Zhang Q., Dagerlind A., Nilsson S., Wiesenfeld-Hallin Z., Hökfelt T. Central and peripheral expression of galanin in response to inflammation. *Neuroscience.* 1995;68(2):563-576.

Johnson M.D., Kao O.E., Kipke D.R. Spatiotemporal pH dynamics following insertion of neural microelectrode arrays. *J Neurosci Methods* 2007;160(2):276-287.

Kar S., Rees R.G., Quirion R. Altered Calcitonin Gene-related Peptide, Substance P and Enkephalin Immunoreactivities and Receptor Binding Sites in the Dorsal Spinal Cord of the Polyarthritic Rat. *Eur J Neurosci.* 1994;6(3):345-354.

Kinney J.W. Starosta G., Holmes A., Wrenn C.C., Yang R.J., Harris A.P., Long K.C., Crawley J.N. Deficits in trace cued fear conditioning in galanin-treated rats and galanin-overexpressing transgenic mice. *Lear Mem.* 2002;9(4):178-190.

Köhler P., Wolff A., Ejserholm F., Wallman L., Schouenborg J., Linsmeier C.E. Influence of probe flexibility and gelatin embedding on neuronal density and glial responses to brain implants. *PloS One.* 2015;10(3):e0119340.

Koltzenburg M., Wall P.D., McMahon S.B. Does the right side know what the left is doing? *Trends in Neuroscience.* 1999;22(3):122-127.

Krukoff T.L. Expression of c-fos in studies of central autonomic and sensory systems. *Mol Neurobiol.* 1994;7(3-4):247-263.

Lang R., Gundlach A.L., Holmes F.E., Hobson S.A., Wynick D., Hökfelt T., Kofler B. Physiology, signaling, and pharmacology of galanin peptides and receptors: three decades of emerging diversity. *Pharmacol Rev.* 2015;67(1):118-175.

Lang R., Kofler B. The galanin peptide family in inflammation. *Neuropeptides.* 2011;45(1):1-8.

Le Bars D., Gozariu M., Cadden S.W. Animal models of nociception. *Pharmacology Review.* 2001;53(4):597-652.

Leah J., Menétrey D., De-Pommery J. Neuropeptides in long ascending spinal tract cells in the rat: evidence for parallel processing of ascending information. *Neuroscience.* 1988;24:195-207.

Li J.H., Wang Y.H., Wolfe B.B., Krueger K.E., Corsi L., Stocca G., Vicini S. Developmental changes in localisation of NMDA receptor subunits in primary cultures of cortical neurons. *Eur J Neurosci.* 1998;10(5):1704-1715.

Li J.L., Kaneko T., Shigemoto R., Mizuno N. Distribution of trigeminohypothalamic and spinohypothalamic tract neurons displaying substance P receptor-like immunoreactivity in the rat. *J Comp Neurol.* 1997;378(4):508-521.

Lind G., Linsmeier C.E., Thelin J., Schouenborg J. Gelatine-embedded electrodes--a novel biocompatible vehicle allowing implantation of highly flexible microelectrodes. *Neural engineering.* 2010;7(4): 046005. doi: 10.1088/1741-2560/7/4/046005.

Ling L.J., Honda T., Shimada Y., Ozaki N., Shiraishi Y., Sugiura Y. Central projection of unmyelinated (C) primary afferent fibers from gastrocnemius muscle in the guinea pig. *J Comp Neurol.* 2003;461(2):140-150.

Liu H.X., Hökfelt T. The participation of galanin in pain processing at the spinal level. *Trends Pharmacol Sci.* 2002;23(10):468-474.

Liu J., Dalmau J., Szabo A., Rosenfeld M., Huber J., Furneaux H. Paraneoplastic encephalomyelitis antigens bind to the AU-rich elements of mRNA. *Neurology.* 1995;45(3 Pt 1):544-550.

Liu P.C., Zhou, J., Li S.L., Ma, H.M. Review of microelectrode fabrication. *Advanced Materials Research.* 2012;565.

Ljungdahl A., Hökfelt T., Nilsson G., Goldstein M. Distribution of substance P-like immunoreactivity in the central nervous system of the rat--II. Light microscopic localization in relation to catecholamine-containing neurons. *Neuroscience.* 1978;3(10):945-976.

Ljungquist B., Jensen T., Etemadi L., Thelin J., Lind G., Garwicz M., Petersson P., Tsanakalis F., Schouenborg J. Discrepancies between cortical and behavioural long-termreadou ts of hyperalgesia in awake freely moving rats. *Eur J of Pain.* 2016;20(10):1689-1699.

Lopes D.M., McMahon S.B. Ultraviolet Radiation on the Skin: A painful experience? *CNS Neurosci Ther.* 2016;22(2):118-126.

Loyd D.R. Anne Z.Murphy. Review article: The role of the periaqueductal gray in the modulation of pain in males and females: are the anatomy and physiology really that different? *Neural Plast.* 2009:462879.

Lundberg D., Axelsson S. Behandling av långvarig smärta - en systematisk litteraturöversikt. SBUs sammanfattning och slutsatser (Treatment of chronic pain--a systematic literature review. SBU's summary and conclusions). *Läkartidningen (The Journal of the Swedish Medical Association).* 2006;103(17):1297-1303.

Mantyh P.W., DeMaster E., Malhotra A., Ghilardi J.R., Rogers S.D., Mantyh C.R., Liu H., Basbaum A.I., Vigna S.R., Maggio J.E., et al. Receptor endocytosis and reshaping of spinal neurons after somatosensory stimulation. *Science.* 1995;268(5217):1629-1632.

Mapp P.I., Terenghi G., Walsh D.A., Chen S.T., Cruwys S.C., Garrett N., Kidd B.L., Polak J.M., Blake D.R. Monoarthritis in the rat knee induces bilateral and time-dependent

changes in substance P and calcitonin gene-related peptide immunoreactivity in the spinal cord. *Neuroscience.* 1993;57(4):1091-1096.

Marusich M.F., Furneaux H.M., Henion P.D., Weston J.A. Hu neuronal proteins are expressed in proliferating neurogenic cells. *J Neurobiol.* 1994;25(2):143-155.

Menétrey D., Chaouch A., Binder D., Besson J.M. The origin of the spinomesencephalic tract in the rat: an anatomical study using the retrograde transport of horseradish peroxidase. *J Comp Neurol.* 1982;206(2):193-207.

Mullen R.J., Buck C.R., Smith A.M. NeuN, a neuronal specific nuclear protein in vertebrates. *Development.* 1992;116(1):201-211.

Nahin R.L., Madsen A.M., Giesler GJ J.r. Anatomical and physiological studies of the gray matter surrounding the spinal cord central canal. *J Comp Neurol.* 1983;220(3):321-335.

Nazli M., Morris R. Comparison of localisation of the neurokinin 1 receptor and nitric oxide synthase with calbindin D labelling in the rat spinal cord. *Anat Histol Embryol.* 2000;29(3):141-143.

Noguchi K., Morita Y., Kiyama H., Ono K., Tohyama M. A noxious stimulus induces the preprotachykinin-A gene expression in the rat dorsal root ganglion: a quantitative study using in situ hybridization histochemistry. *Brain Res.* 1988;464(1):31-35.

Nolta N.F., Christensen M.B., Crane P.D., Skousen J.L., Tresco P.A. BBB leakage, astrogliosis, and tissue loss correlate with silicon microelectrode array recording performance. *Biomaterials*. 2015;53:753-762.

O'Neill J., Sikandar S., McMahon S.B., Dickenson A.H. Human psychophysics and rodent spinal neurones exhibit peripheral and central mechanisms of inflammatory pain in the UVB and UVB heat rekindling models. *J Physiol.* 2015;593(17):4029-4042.

Obeso J.A., Olanow C.W., Rodriguez-Oroz M.C., Krack P., Kumar R., Lang A.E. Deep-brain stimulation of the subthalamic nucleus or the pars interna of the globus pallidus in Parkinson's disease. *N Engl J Med.* 2001;345(13):956-963.

Olave M.J., Maxwell D.J. Axon terminals possessing α2c-adrenergic receptors densely innervate neurons in the rat lateral spinal nucleus which respond to noxious stimulation. *Neuroscience.* 2004;126(2):391-403.

Olson B.R. Freilino M., Hoffman G.E., Stricker E.M., Sved A.F., Verbalis J.G. c-Fos Expression in rat brain and brainstem nuclei in response to treatments that alter food intake and gastric motility. *Mol Cell Neurosci.* 1993;4(1):93-106.

Petkó M., Antal M. Propriospinal afferent and efferent connections of the lateral and medial areas of the dorsal horn (laminae I-IV) in the rat lumbar spinal cord. *J Comp Neurol.* 2000;422(2):312-325.

Phillips R.J., Hargrave S.L., Rhodes B.S., Zopf D.A., Powley T.L. Quantification of neurons in the myenteric plexus: an evaluation of putative pan-neuronal markers. *J Neurosci Methods.* 2004;133(1-2):99-107.

Polgár E., Szûcs P., Urbán L., Nagy I. Alterations of substance P immunoreactivity in lumbar and thoracic segments of rat spinal cord in ultraviolet irradiation induced hyperalgesia of the hindpaw. *Brain Res.* 1998;786(1-2):248-251.

Portiansky E.L., Barbeito C.G., Gimeno E.J., Zuccolilli G.O., Goya R.G. Loss of NeuN immunoreactivity in rat spinal cord neurons during aging. *Exp Neurol.* 2006;202(2):519-521.

Ramos-Vara J.A. Technical aspects of immunohistochemistry. *Vet Pathol.* 2005;42(4):405-426.

Rethelyi M. Neurons of the lateral spinal nucleus in the rat spinal cord - A Golgi study. *Eur J Anat.* 2003;7(1):1-8.

Rea P.M. The role of the lateral spinal nucleus in nociception. PhD- Thesis. Thesis, University of Glasgow, Glasgow, UK, 2009, http://theses.gla.ac.uk/1029/.

Rexed B., Brodal A. The nucleus cervicalis lateralis: a spino-cerebellar relay nucleus. *J Neurophysiol.* 1951;14:399-407.

Rukwied R., Dusch M., Schley M., Forsch E., Schmelz M. Nociceptor sensitization to mechanical and thermal stimuli in pig skin in vivo. *Eur J Pain.* 2008;12(2):242-250.

Saadé N.E., Farhat O., Rahal O., Safieh-Garabedian B., Le Bars D., Jabbur S.J. Ultra violet-induced localized inflammatory hyperalgesia in awake rats and the role of sensory and sympathetic innervation of the skin. *Brain Behav Immun.* 2008;22(2):245-256.

Schmidt E.M. Mcintosh J.S., Bak M.J. Long-term implants of Parylene-C coated microelectrodes. *medical and biological engineering and computing.* 1988;26(1):96-101.

Schnitzler A., Ploner M. Neurophysiology and functional neuroanatomy of pain perception. *clinical neurophysiology.* 2000;17(6):592-603.

Seiffert K., Granstein RD. Neuropeptides and neuroendocrine hormones in ultraviolet radiation-induced immunosuppression. *Methodes.* 2002;28(1):97-103.

Senba E., Shiosaka S., Hara Y., Inagaki S., Sakanaka M., Takatsuki K., Kawai Y., Tohyama M. Ontogeny of the peptidergic system in the rat spinal cord. *J Comp Neurol.* 1982;208(1):54-66.

Sergeyev V., Broberger C., Hökfelt T. Effect of LPS administration on the expression of POMC, NPY, galanin, CART and MCH mRNAs in the rat hypothalamus. *Brain Res Mol Brain Res.* 2001;90(2):93-100.

Shenker N., Haigh R., Roberts E., Mapp P., Harris N., Blake D. A review of contralateral responses to a unilateral inflammatory lesion. *Rheumatology.* 2003;42(11):1279-1286.

Shi T.J., Cui J.G., Meyerson B.A., Linderoth B., Hökfelt T. Regulation of galanin and neuropeptide Y in dorsal root ganglia and dorsal horn in rat mononeuropathic models: possible relation to tactile hypersensitivity. *Neuroscience.* 1999;93(2):741-757.

Solodkin A., Traub R.J, Gebhart G.F. Unilateral hindpaw inflammation produces a bilateral increase in NADPH-diaphorase histochemical staining in the rat lumbar spinal cord. *Neuroscience.* 1992;51(3):495-499.

Suyatin D.B., Wallman L., Thelin J., Prinz C.N., Jörntell H., Samuelson L., Montelius L., Schouenborg J. Nanowire-based electrode for acute in vivo neural recordings in the brain. *PloS One.* 2013;8(2): e56673. doi: 10.1371/journal.pone.0056673.

Szabo A., Dalmau J., Manley G., Rosenfeld M., Wong E., Henson J., Posner J.B., Furneaux H.M. HuD, a paraneoplastic encephalomyelitis antigen, contains RNA-binding domains and is homologous to Elav and Sex-lethal. *Cell.* 1991;67(2):325-333.

Szentágothai J. Neuronal and synaptic arrangement in the substantia gelatinosa rolandi. *J Comp Neurol.* 1964;122:219-239.

Takayama K., Suzuki, T., Miura, M. The comparison of effects of various anesthetics on expression of Fos protein in the rat brain. *Neurosci Lett.* 1994;176(1):59-62.

Todd A.J., Puskar Z., Spike R.C., Hughes C., Watt C., Forrest L. Projection neurons in lamina I of rat spinal cord with the neurokinin 1 receptor are selectively innervated by substance-P containing afferents and respond to noxious stimulation. *J Neurosci.* 2002;22(10):4103-4113.

Todd A.J., Spike, R.C., Young, S., Puskár, Z. Fos induction in lamina I projection neurons in response to noxious thermal stimuli. *Neuroscience.* 2005;131(1):209-217.

Valtschanoff J.G., Weinberg R.J., Rustioni A., Schmidt H.H. Nitric oxide synthase and GABA co-localise in lamina II of rat spinal cord. *Neurosci Lett.* 1992;148(1-2):6-10.

Villar M.J., Cortés R., Theodorsson E., Wiesenfeld-Hallin Z., Schalling M., Fahrenkrug J., Emson P.C., Hökfelt T. Neuropeptide expression in rat dorsal root ganglion cells and spinal cord after peripheral nerve injury with special reference to galanin. *Neurosciece.* 1989;33(3):587-604.

von Banchet S.G., Petrow P.K., Bräuer R., Schaible H.G. Monoarticular antigen-induced arthritis leads to pronounced bilateral up-regulation of the expression of neurokinin 1 and bradykinin 2 receptors in dorsal root ganglion neurons of rats. *Arthritis Res.* 2000;2(5):424-427.

Willis Jr W.D., Coggeshall R.E. Chapter 8: Sensory pathways in the dorsal lateral funiculus (pp. 307–340) in Sensory Mechanisms of the Spinal Cord, 2nd edition, 1999, Plenum Press, New York and London, ISBN: 0-306-43781-3.

Woolf C.J. Overcoming obstacles to developing new analgesics. *Nat Med.* 2010;16(11):1241- 1247.

LUND UNIVERSITY
Faculty of Medicine